and downstream regions of the *com* genes were amplified with pairs of primers (Table 2), using chromosomal DNA from UA159 as a template. Initially, PCR products of the upstream region of *comC* (*comCA*) were cloned into plasmid pUC19. Next, PCR products of the downstream regions of *comC* (*comCB*) were ligated to *comCA*. The resultant plasmid was digested with *Bam*HI, after which *Bam*HI-digested pResEmMCS10 (41) was inserted. The chimeric plasmid was then linearized with *Eco*RI and the linear plasmid was used to transform *S. mutans* UA159. The plasmids for inactivating the *comD*, *comE*, and *comX* mutants were constructed in a similar manner as for the *comC* mutant. Confirmation of plasmid insertions causing gene disruption was performed by either Southern blotting or PCR (data not shown). ComCAF and ComCBR, ComXAF and ComXBR, ComDAF and ComDBR, and ComEAF and ComEBR in Table 2 were used for PCR as *comC*, *comX*, *comD*, and *comE* mutant plasmids.

Extraction of RNA

Total RNA was isolated from 1.0 ml log-phase cell cultures for 4 h with or without CSP treatment and a slight modification of the RNeasy Mini Kit protocol (Qiagen GmbH, Hilden, Germany) using on-column DNase digestion with RNase-free DNase I (Qiagen). Briefly, the harvested samples were resuspended in 100 μl TE (10 mM Tris-HCl 1 mM EDTA pH 8.0) buffer containing 6 μl lysozyme (50 mg/ml) and 40 U of mutanolysin, followed by incubation at 37°C for 60 min. The soluble samples were treated using a RNeasy Mini Kit according to the directions of the supplier.

Transcription analysis

To confirm whether the expression of *glrA* is dependent on the quorum sensing systems of *com* genes in *S. mutans*, reverse transcription-PCR (RT-PCR) analysis was performed. An overnight culture of the *S. mutans* UA159Δ*comC* was diluted 100-fold in fresh medium and grown at 37°C. After 180, 210, 225, or 235 min of growth, CSP was added to a final concentration of 0.2 μM for each culture. After a total of 4 h incubation, all cultures were used for RNA isolation. For RT-PCR analysis, 1 μg RNA from each sample was used and RT-PCR was performed using the SuperScript III first-strand synthesis system (Invitrogen Corp., Carlsbad, CA) with a random primer (Invitrogen) according to the recommended procedures. First, to check for DNA contamination in the samples, purified total RNA without reverse transcription was used as a negative control for PCR with a pair of universal and *glrA* primers (data not shown). PCR was then performed using the synthesized complementary DNA indicated as templates and primers. The *glrA* primers of *S. mutans* open reading frames (forward: GCGATCAAAGAATTTCGGC, reverse: CAAACGCCAAGATTTAGAA) were used to detect *glrA* expression. The RT-PCR results were normalized using the 16S ribosomal RNA sequences of gram-positive bacteria primers as internal controls (24).

Bacteriocin assay

To clarify the effects of sub-purified culture supernatant samples from *S. salivarius* HT9R on CSP activity, 18 μl culture supernatant (0, 3.125, 6.25, 12.5, 25.0, 50.0, and 100.0 μg/ml) filtered through 0.22-μm pore-size filters was mixed and incubated with 2 μl exogenous CSP (1 mM) at 37°C for 1 h. Then, 4 μl CSP solution treated in this way was added to *S. mutans* UA159Δ*comC* (0.9×10^4 CFU) in 36 μl fresh TSBS to a final concentration of 10 μM CSP and incubated on the BHI 1% agar (Wako, Tokyo, Japan) plate at 37°C for 24 h. The indicator strain RP66 was grown to an optical density of 0.3 at 550 nm. Each culture was then diluted to 1 : 100 and 0.2 ml of the dilution was transferred by pipette into a tube containing 4 ml molten BHI with 1% agar. The solution was mixed and poured evenly onto the surfaces of the plates, then at 37°C for an additional 24 h, after which the diameters of the zones of inhibition were measured.

To measure CSP production levels by *S. mutans* FSC-3 and FSC-3Δ*glrA*, *S. mutans* GS5 and GS5Δ*comC* were used. Recently, it was reported that the addition of exogenous CSP to *S. mutans* GS-5Δ*comC* in a plate assay using indicator strain RP66 restored the ability to produce bacteriocin (46). The production of CSP from *S. mutans* FSC-3 and FSC-3Δ*glrA* was indicated by the inhibition zones based on bacteriocin produced from *S. mutans* GS-5Δ*comC* in plate assays of *S. mutans* GS5Δ*comC* mixed separately with *S. mutans* FSC-3 and FSC-3Δ*glrA*. Loopfuls of stationary-phase cultures of the *Streptococcus* strains were stabbed into BHI agar on a plate, and then incubated under anaerobic conditions at 37°C for 6 or 24 h. The indicator strain RP66 was also grown and used to measure the diameters of the zones of inhibition revealed by the above-described method.

Transformation assays

Transformation efficiency was measured as previously described with minor modifications (1). Briefly, overnight cultures of *S. mutans* UA159 were diluted 1 : 20 in BHI medium containing horse serum (10%, volume/volume). A 0.2-ml aliquot of the cultures was incubated at 37°C for 2 h in a microcentrifuge tube (BIO-BIK, Osaka, Japan) and then added with or without 2 μl synthetic CSP solution (1 μmol/ml), which was treated with 0, 6.25, 12.5, 25.0, 50.0, or 100.0 μg/ml sub-purified culture supernatant sample from *S. salivarius* HT9R for 1 h at 37°C, and overnight culture supernatants of *S. mutans* UA159, FSC-3 or FSC-3Δ*glrA* (1/40 or 1/80 dilution in final concentration). After incubation for 30 min to allow the induction of competence, the cultures were exposed to 200 ng plasmid pDL 276. After 3 h at 37°C, cultures were chilled on ice and transformants and total CFU were enumerated by plating cells in BHI agar plates with or without 500 ng/ml kanamycin. Transformation efficacy was determined after 48 h of incubation and was expressed as the percentage of transformants among the total viable recipient cells.

Statistical analysis

Comparisons of biofilm formation levels among the various cultures of *S. mutans* UA159 and UA159Δ*comC* and transformations of plasmid into *S. mutans* UA159 treated with various stimulators were performed by Fisher's protected least significant difference and analysis of variance. A *P*-value of 0.01 or less was considered to indicate statistical significance.

Results

Biofilm formation with dual-species cultures in 96-well microtiter plates

To evaluate the abilities of *S. salivarius* to form biofilms with *S. mutans*, combination cultures of *S. mutans* and *S. salivarius* were grown in 96-well microtiter plates coated with salivary components. The inhibiting effects of *S. salivarius* in dual-species cultures with *S. mutans* GS5 were observed at various time-points (Fig. 1A). Inhibition was recognized at 4 and 8 h after the start of culturing. Each of the culture supernatants, except for the single culture with HT9R, had

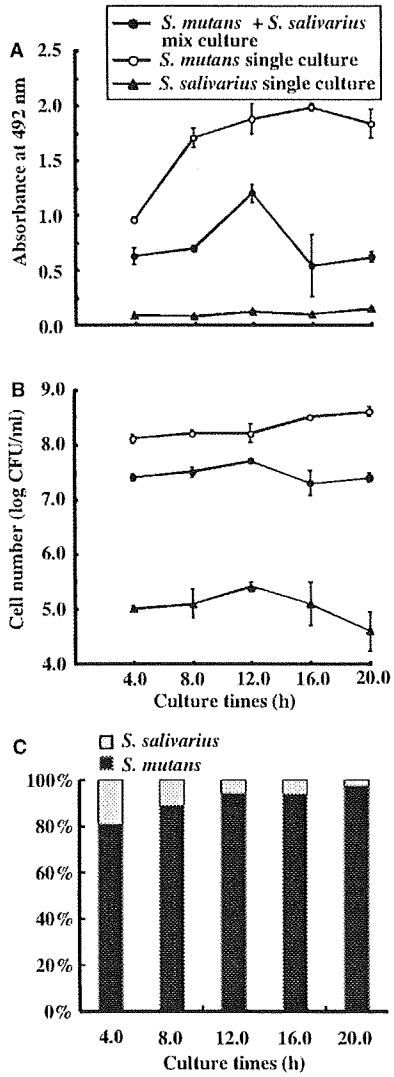

Fig. 1. Formation of biofilms by dual-species cultures at various time-points. Graphs show quantification of biofilms formed after 4, 8, 12, 16, and 20 h in cultures of *Streptococcus mutans* GS5 and *Streptococcus salivarius* HT9R in a 96-well microtiter plate (A), colony-forming units (CFU)/biofilm in a 24-well microtiter plate (B) and proportion of *S. mutans* GS-5 or *S. salivarius* HT9R in biofilm (C). The culture conditions were divided into the following three groups: (i) simultaneous culture of GS5 and *S. salivarius*, (ii) single culture of GS5, and (iii) single culture of *S. salivarius*. The results are expressed as the mean ± SD of absorbance at 492 nm obtained in triplicate assays. Representative data from three independent experiments are presented, with similar results obtained in each.

a pH level of around 6.0 after 4 h, while pH levels in the range of 4.6–4.9 were found in the other experiments after 4 h. At all time-points, the total number of cells in the biofilm was lower in the dual-species cultures compared with the single species culture with *S. mutans*, while the number was higher than that in the single species culture of *S. salivarius* (Fig. 1B). Furthermore, the proportion of *S. mutans* cells in the biofilms was greater than 80% after 4 h and then continued to slightly increase until 20 h (Fig. 1C). These results indicate that *S. salivarius* had inhibiting effects on subsequent biofilm growth and cell numbers of *S. mutans* after 4 h of dual-species culture. To confirm whether *S. salivarius* produced a substance that inhibited the biofilm formation of *S. mutans*, the culture supernatant from *S. salivarius* was sub-purified by gel filtration. The sub-purified sample significantly inhibited biofilm formation in a dose-dependent manner (Fig. 3).

Relationship between biofilm inhibition by *S. salivarius* and CSP

Wang and Kuramitsu reported that some oral streptococci, including *S. gordonii*, *S. sanguinis*, *S. mitis*, and *S. oralis*, have an ability to inactivate *S. mutans* CSP (46). It was also speculated that CSP is inactivated by *S. salivarius* HT9R, while destruction of the CSP-dependent quorum sensing system has been associated with the inhibition of biofilm formation by *S. salivarius* in dual cultures. To clarify the situation, *S. mutans* UA159Δ*comC* was constructed and used for the biofilm formation assay using a pretreatment sample of CSP with the sub-purified sample. Before the biofilm formation assay, the growth of *S. mutans* UA159 and UA159Δ*comC* was studied in the presence of CSP. Addition of exogenous CSP inhibited continuously the cell growth of *S. mutans* UA159 after 8 h of culture (Fig. 2A). In contrast, the cell growth of *S. mutans* UA159Δ*comC* was inhibited by the addition of CSP at 8 h but was restored to the growth level found in conditions without CSP after 10 h of culture (Fig. 2B). It is proposed that the difference in cell growth between *S. mutans* wild-type and the *comC* mutant in the presence of CSP is because the originating CSP from wild-type may combine with the continuous inhibition of cell growth of *S. mutans* UA159 by CSP during 16 h of culture, but the cell growth of *S. mutans* UA159Δ*comC* is only temporarily inhibited by the limiting amount of added CSP under the condition with no originating CSP. As a result, the cell growth of *S. mutans* UA159Δ*comC* in the presence of CSP was similar to that in conditions without CSP by 16 h after incubation.

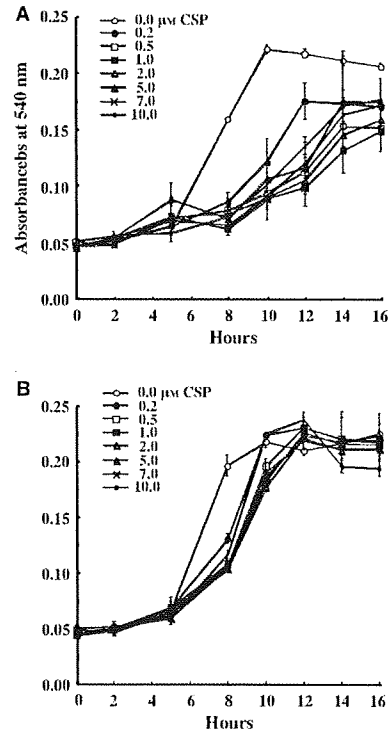

Fig. 2. Cell growth of *Streptococcus mutans* UA159 and UA159Δ*comC* in culture with competence-stimulating peptide (CSP). Graphs show quantification of cell growth after 0, 2, 5, 8, 10, 12, 14, and 16 h in culture of *S. mutans* UA159 (A) or UA159Δ*comC* (B) with 0, 0.2, 0.5, 1.0, 2.0, 5.0, 7.0, and 10.0 μM CSP. The results are expressed as the mean ± SD of absorbance at 540 nm obtained in triplicate assays. Representative data from three independent experiments are presented, with similar results obtained in each.

To clarify the inhibition mechanism of *S. salivarius*, CSP was pretreated with a sub-purified culture supernatant sample from *S. salivarius*, and then added to an *S. mutans* UA159Δ*comC* culture and incubated in plates for 16 h. Biofilm formation by the *comC* mutant was significantly inhibited by pretreatment with the CSP-added supernatant sample and the sub-purified sample could not inhibit biofilm formation by *S. mutans* UA159Δ*comC* without CSP (Fig. 3). To obtain clear details of the inhibitory effect of the sub-purified sample, bacteriocin production of *S. mutans* GS-5Δ*comC* and transformation of pDL276 (Ka^r) into *S. mutans* UA159 in the presence of CSP, which is another CSP-dependent biological system (1, 47), was also utilized. Bacteriocin production and transformation were clearly and significantly inhibited by pretreatment with the CSP-added supernatant sample in a dose-dependent manner

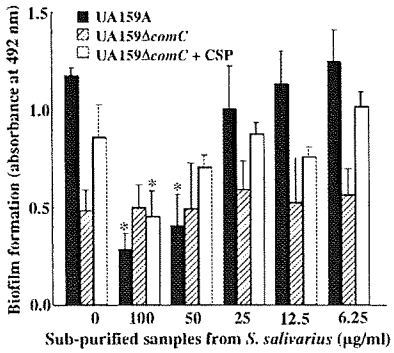

Fig. 3. Biofilm formation by *Streptococcus mutans* with culture supernatant from *Streptococcus salivarius*. Graphs show quantification of biofilms formed after 16 h in separate cultures of *S. mutans* UA159 and UA159Δ*comC* with various concentrations (0, 6.25, 12.5, 25.0, and 50.0 μg/ml) of culture supernatant samples from *S. salivarius* in a 96-well microtiter plate. Competence-stimulating peptide (CSP) pretreatment of supernatants was also used to investigate biofilm formation by UA159Δ*comC*. The results are expressed as the mean ± SD of absorbance at 492 nm obtained in triplicate assays. Representative data from three independent experiments are presented, with similar results obtained in each. Asterisks denote significantly different relative levels of biofilm formation ($P < 0.01$, vs. biofilm of UA159, UA159Δ*comC*, or UA159Δ*comC* + CSP without culture supernatant sample).

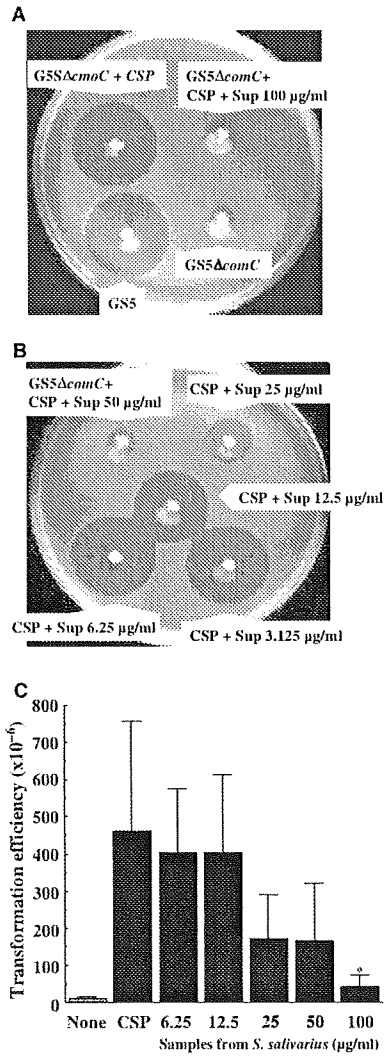

Fig. 4. Bacteriocin production and competence activity by *Streptococcus mutans* with competence-stimulating peptide (CSP) and culture supernatant from *Streptococcus salivarius*. The production of bacteriocin was observed in 24-h cultures of GS-5, GS-5Δ*comC*, and GS-5Δ*comC* added with CSP solutions after preincubation with CSP and culture supernatant sample (3.125, 6.25, 12.5, 25.0, 50.0, 100.0 μg/ml) from *S. salivarius* HT9R (A and B). The streptococcal strain RP66 was used as an indicator strain. Representative data from three independent experiments were presented. pDL276 (Ka^r) was transformed into *S. mutans* UA159 stimulated with or without CSP which was treated with 0, 6.25, 12.5, 25.0, 50.0, and 100.0 μg/ml of sub-purified culture supernatant sample from *S. salivarius*. Transformation frequency was determined from the ratio of the number of transformants vs. that of the total viable recipients, multiplied by 100 (C). The results were obtained from three independent assays and are expressed as the mean ± SD. Asterisks denote significantly different relative levels of transformation [$P < 0.05$, vs. transformation efficacy in *S. mutans*-treated CSP (1 μmol)].

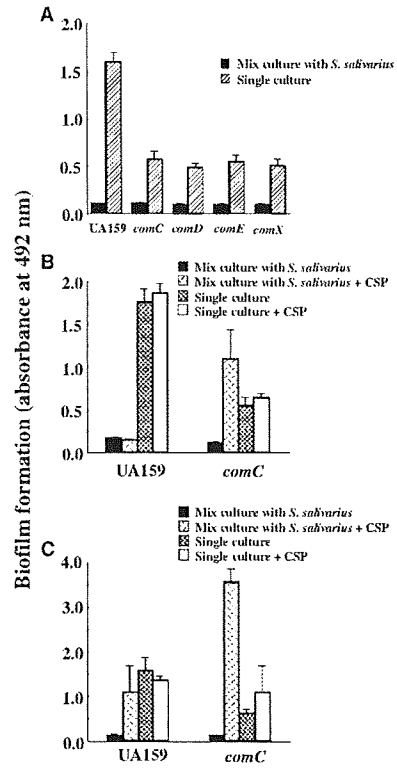

Fig. 5. Effects of competence-stimulating peptide (CSP) on biofilm formation by *Streptococcus salivarius* and *Streptococcus mutans*. *S. mutans* UA159, UA159Δ*comC* (comC), UA159Δ*comD* (comD), UA159Δ*comE* (comE), and UA159Δ*comX* (comX) were each incubated with or without *S. salivarius* HT9R (A). UA159 and UA159Δ*comC* were mixed separately with HT9R, after which 1 μM (B) or 10 μM (C) of CSP was added. All mixtures were incubated aerobically for 16 h at 37°C in 96-well microtiter plates. The results are expressed as the mean ± SD of absorbance at 492 nm obtained in triplicate assays. Representative data from three independent experiments are presented, with similar results obtained in each.

(Fig. 4A–C). We therefore considered that biofilm formation was inhibited by CSP inactivation of *S. salivarius*. To analyse still other mechanisms related to the inactivation of CSP in biofilm inhibition, *com* mutants were mixed and cultured with *S. salivarius* cells. The inhibition was greater in the mixed cultures than in the single culture biofilms (Fig. 5A). However, addition of CSP (1 μM) restored biofilm formation in mixed cultures of the *comC* mutant and *S. salivarius* (Fig. 5B). Furthermore, addition of an increased amount (10 μM) of CSP also restored biofilm formation in the mixed cultures of UA159 and the *comC* mutant with *S. salivarius*, and resulted in a more than twofold increase in biofilm formation compared with the wild-type (Fig. 5C).

Influence of *glrA* on biofilm inhibition in dual-species cultures

Based on our results, we also speculated that morphological differences among the *S. mutans* biofilm formations were related to the inhibition of biofilm development in dual-species cultures with *S. salivarius*. Therefore, we compared FSC-3 with FSC-3Δ*glrA* using dual-species cultures to determine the influence of morphological change on that inhibition. *S. salivarius* inhibited biofilm formation when cultured with FSC-3, but not when cultured with FSC-3Δ*glrA* (Fig. 6). To investigate the relationship between *glrA* and the CSP-dependent quorum sensing system, *glrA* was subjected to RT-PCR with various *com* mutants and the *comC* mutant stimulated by CSP. The results showed that *glrA* was expressed in the *comX* mutant, but not in the *comC*, *comD*, and *comE* mutants (Fig. 7A), though expression was observed in the *comC* mutant 15 min after the addition of CSP (Fig. 7B). In contrast, CSP addition did not affect biofilm formations in mixed cultures of FSC-3 and FSC-3Δ*glrA* with *S. salivarius* (Fig. 7C).

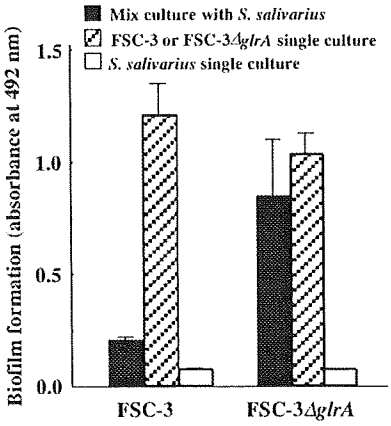

Fig. 6. Biofilm formations by FSC-3 and FSC-3Δ*glrA* with *Streptococcus salivarius*. Graphs show quantification of biofilms formed after 16 h of dual-species cultures of *Streptococcus mutans* FSC-3 (A) and FSC-3Δ*glrA* (B) with *S. salivarius* HT9R in 96-well microtiter plates. The culture conditions were divided into the following three groups: (i) simultaneous culture of FSC-3 or FSC-3Δ*glrA* and other streptococci, (ii) single culture of FSC-3 or FSC-3Δ*glrA*, (iii) single culture of *S. salivarius*. The results are expressed as the mean ± SD of absorbance at 492 nm obtained in triplicate assays. Representative data from three independent experiments are presented, with similar results obtained in each.

These findings demonstrated that *glrA* expression in the CSP-dependent quorum sensing system is associated with susceptibility to biofilm inhibition involved in the inactivation of CSP by *S. salivarius*. However, morphological changes, such as a reduction and accretion of volume in the biofilm bottom and top areas of FSC-3Δ*glrA* on a hard surface in comparison with the wild-type FSC-3 (28), were probably associated with the resistance to inhibition by *S. salivarius*. Moreover, we speculated that there was a greater production of CSP by FSC-3Δ*glrA* than by FSC-3, so *S. salivarius* did not inhibit biofilm formation in the dual-species culture with FSC-3Δ*glrA*.

Influence of *glrA* on CSP-dependent bacteriocin production and genetic transformation assay

To investigate our theory, CSP-dependent bacteriocin production and transformation assays were performed to measure CSP production (1, 47). *S. mutans* GS-5Δ*comC*, which did not show CSP-dependent production of bacteriocin with indicator strain group c streptococcus RP66 cells, was mixed separately with FSC-3 and FSC-3Δ*glrA*, then bacteriocin production was compared between mixed cultures with *S. mutans* GS-5Δ*comC* and FSC-3, or FSC-3Δ*glrA* using plate assays. Greater bacteriocin production was observed in the culture of *S. mutans* GS-5Δ*comC* with FSC-3Δ*glrA* than in that with FSC-3, as indicated by the diameter of the inhibition zone of the indicator strain RP66 (Fig. 7D). However, FSC-3, FSC-3Δ*glrA*, and GS-5Δ*comC* produced minimal amounts of bacteriocin. Furthermore, greater transformation of pDL276 into *S. mutans* UA159 was observed in the culture of *S. mutans* UA159 with 1/40 dilution of culture supernatant from FSC-3Δ*glrA* than in that with FSC-3 (Fig. 7E). These results indicate that FSC-3Δ*glrA* produces greater amounts of CSP than FSC-3.

Discussion

In the present study, we investigated the effects of *S. salivarius* on CSP-dependent biofilm formation by *S. mutans* in 96-well microtiter plates coated with salivary components. Few biofilms were observed in mono-species cultures of *S. salivarius* HT9R, whereas biofilm formation was inhibited in dual-species cultures with *S. mutans*. *S. salivarius* produces substances that inhibit biofilm formation by *S. mutans*. A prepared culture supernatant sample from *S. salivarius* played a role in the inactivation of CSP, although it was not able to inhibit biofilm formation by UA159Δ*comC* without CSP, it did inhibit biofilm formation by *S. mutans* UA159Δ*comC* and bacteriocin production and transformation of pDL276 into *S. mutans* UA159 after preculturing with CSP (Figs 3 and 4). Furthermore, the addition of CSP restored biofilm formation in dual-species cultures of UA159 and UA159Δ*comC* with *S. salivarius* (Fig. 5B,C).

The inhibition by *S. salivarius* observed in our experiments was not dependent on acid produced by the oral streptococci because the pH levels in the supernatants after culturing were similar in all cultures and the supernatant sample from *S. salivarius* inhibited biofilm formation, although it did not have an influence on culture pH (Fig. 3). We found at least four proteins in the supernatant sample, estimated to range in size from 97.4 to 200 kDa, in a sodium dodecyl sulfate–polyacrylamide gel electrophoresis (SDS–PAGE) assay that utilized Coomassie blue staining (data not shown). The sample did not include the molecular mass (62 kDa) of the large subunit of urease from *S. salivarius* (7). In addition, the *S. salivarius* strain did not produce bacteriocin against *S. mutans* (data not shown). Taken together, our results indicate that the inhibiting substance of *S. salivarius* reacts with CSP to inhibit the development of biofilm formation. Furthermore, it is not an antimicrobial agent, such as acid or bacteriocin that causes direct injury to *S. mutans* cells or a biological agent such as urease.

It is generally considered that the mechanisms employed by healthy microflora to interfere with the adhesion of invading pathogens include competitive exclusion (38), displacement (27), production of antibacterial compounds (15), and the release of biosurfactants (11). Recently, some investigators have proposed quorum sensing systems and virulence response as new targets for strategies to reduce the cariogenicity of organisms such as *S. mutans* (46, 48). Factors such as acid tolerance (47), genetic competence (22), and bacteriocin production (47) in those quorum sensing systems may be modulated by interspecies communication between cariogenic and other types of bacteria in oral biofilms. Another study found that biofilm formation by a *luxS* mutant of *S. mutans* GS5 was complemented by auto-inducer-2 (AI-2) produced by *S. gordonii*, but not that produced by *S. sanguinis* 10556 or *S. salivarius* HT9R (48). However, *S. salivarius* had a two-fold greater level of AI-2 activity than *S. mutans* GS5 in the luminescence assay using *Vibrio harveyi* BB170 and they also noted that additional factors were expressed by some streptococci, which also modulated AI-2 activity. AI-2 plays a role in interspecies signaling, and its concentration was found to be critical for mutualism between *S. oralis* and *Actinomyces naeslundii* grown under conditions that are representative of the human oral cavity (39). In another report, *S. sanguinis* 10556, *S. gordonii* 10558, and *S. mitis* 10712 inhibited bacteriocin production from *S. mutans* GS5, whereas bacteriocin production by *S. mutans* GS5Δ*comC* was restored with the addition of exogenous CSP (46). In the present study, CSP-dependent biofilm formation was also inhibited by *S. salivarius* HT9R. Therefore, auto-inducers including CSP may be target factors for the regulation of biofilm formation by multiple oral streptococci.

To determine whether the ComDE two-component signal transduction system or the alternative sigma factor ComX in addition to ComC, are required for biofilm formation and biofilm inhibition by *S. salivarius*, we performed the single biofilm formation with *comC*, *comD*, *ComE*, and *conX* mutants, and dual-

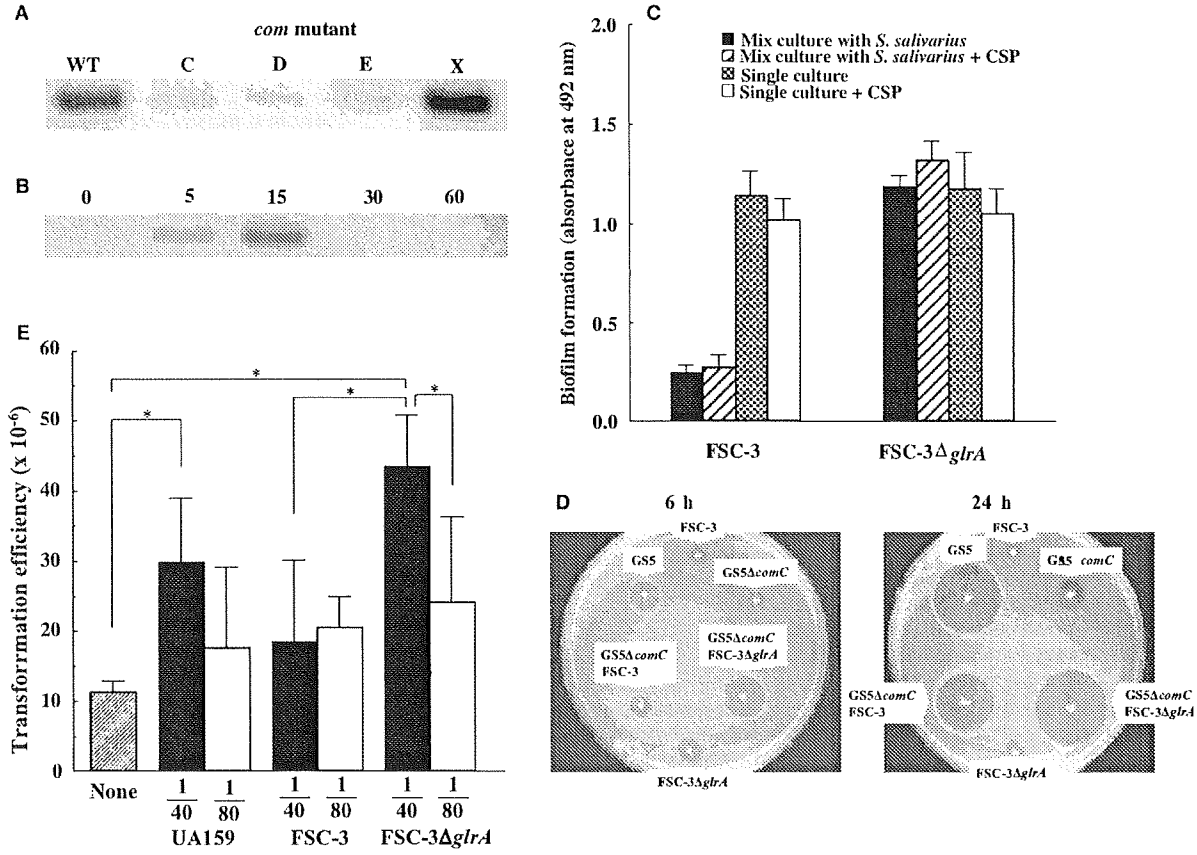

Fig. 7. Contribution of *glrA* to competence-stimulating peptide (CSP)-dependent biofilm formation. Reverse transcription-polymerase chain reaction (RT-PCR) analysis of *glrA* transcription was performed in log-phase culture without CSP of UA159 (wild-type; WT), UA159Δ*comC* (comC), UA159Δ*comD* (comD), UA159Δ*comE* (comE), and UA159Δ*comX* (comX) (A). An RNA sample isolated from UA159Δ*comC* at 0, 5, 15, 30, and 60 min after the addition of 0.2 μM CSP was subjected to RT-PCR with *glrA* (B). FSC-3 and FSC-3Δ*glrA* were each mixed with or without HT9R, with 0.2 μM CSP added. All mixtures were incubated for 16 h at 37°C under 5% CO_2 aerobic conditions in 96-well microtiter plates (C). The results are expressed as the mean ± SD of absorbance at 492 nm obtained in triplicate assays. The production of bacteriocin was observed after 6 and 24 h of single species cultures of FSC-3, FSC-3Δ*glrA*, GS5, and GS5Δ*comC*, and after dual-species cultures of GS-5Δ*comC* and FSC-3, and GS-5Δ*comC* and FSC-3Δ*glrA* (D). The streptococcal strain RP66 was used as an indicator strain. Representative data from three independent experiments are presented, with similar results obtained in each. pDL276 (Ka^r) was transformed into *Streptococcus mutans* UA159 stimulated with or without culture supernatant samples (1/40 and 1/80 dilution in final concentration) from *S. mutans* UA159, FSC-3 and FSC-3Δ*glrA* (E). Transformation frequency was determined from the ratio of the number of transformants vs. that of the total viable recipients, multiplied by 100. The results were obtained from four independent assays and are expressed as the mean ± SD. Asterisks denote significantly different relative levels of transformation ($P < 0.01$).

species biofilm formation with the mutants and *S. salivarius*. These results indicated that the CSP-dependent regulatory systems were involved with the biofilm inhibition of *S. mutans*. *S. salivarius* produces an inhibiting factor for the biofilm formation of *S. mutans*, but dual-species biofilm formation was poor and lower than that for single biofilm of these mutants. Therefore, *S. salivarius* may have other inhibiting mechanisms in addition to CSP inactivation.

Dual-species cultures of *S. salivarius* and the *S. mutans* clinical strain FSC-3 had poor biofilm development, whereas those produced in cultures with the *glrA*-deficient mutant, which is regulated by CSP in the quorum sensing system, were substantial. These findings indicate that the interactions between *glrA* in *S. mutans* and CSP-inhibiting substances from *S. salivarius* might be significantly associated with susceptibility to biofilm inhibition by *S. salivarius*. Our results also suggest that *glrA* is expressed by CSP, inhibits CSP production, and regulates biofilm formation in mixed cultures of *S. mutans* and *S. salivarius*. Therefore, *glrA* may respond to excess CSP or to inactivation of CSP by *S. salivarius*, and regulate CSP production and biofilm formation during autoregulation of the *com*-dependent quorum sensing system. In contrast, that resistance to inhibition by *S. salivarius* may not be dependent on morphological changes, because an increase in CSP may relate to the change in biofilm mass in the bottom and top areas of biofilms formed on a hard surface by FSC-3Δ*glrA* and the inhibition occurred in the early phase of biofilm formation. Therefore, the interaction between the regulation system by *glrA* of CSP and CSP inactivation by the inhibiting substance is an important function for cell-to-cell communication between biofilm-forming bacteria such as *S. mutans* and commensal streptococci such as *S. salivarius*.

Several genes involved in biofilm formation have been identified in a variety of organisms (22, 28, 36, 37, 39, 49), though little is known regarding the responsible substances in biofilm formations with mixed species cultures (39, 45, 46). In the present dual-species experiments, we found that the *glrA* gene was associated with susceptibility to biofilm inhibition by

commensal bacteria and was involved in regulating the production of CSP in cariogenic bacteria. However, scant information is available regarding the mechanisms that are involved with transducing CSP signals between *glrA* and other genes or proteins that control biofilm development. Therefore, definitive conclusions regarding the molecular mechanisms used to control the development of biofilms formed by a mixture of species require further investigation to determine how these signals are sensed and how they interact with *glrA* in biofilm-forming bacteria, as well as to elucidate other possible inhibitors of biofilm streptococci.

Acknowledgments

The authors thank Masayuki Kumada and Kentaro Okuda for their technical support. This work was supported in part by grants-in aid for Development Scientific Research (15390571, 19659559, and 18592011) from the Ministry of Education, Science, and Culture of Japan, and the Ministry of Health, Labour and Welfare (H16-Medical Services-014).

References

1. Ahn SJ, Wen SJ, Burne RA. Multilevel control of competence development and stress tolerance in *Streptococcus mutans* UA159. Infect Immun 2006: **74**: 1631–1642.
2. Aas JA, Paster BJ, Stokes LN, Olsen I, Dewhirst FE. Defining the normal bacterial flora of the oral cavity. J Clin Microbiol 2005: **43**: 5721–5732.
3. Aspiras MB, Ellen RP, Cvitkovitch DG. ComX activity of *Streptococcus mutans* growing in biofilms. FEMS Microbiol Lett 2004: **238**: 167–174.
4. Bowden GH, Ellwood DC, Hamilton IR. Microbial ecology of the oral cavity. In: Alexander M, ed. Advances in microbial ecology, New York: Plenum Press, Vol. 3, 1979: 135–217.
5. Burne RA. Oral streptococci. Products of their environment. J Dent Res 1998: **77**: 445–452.
6. Cain BD, Norton PJ, Eubanks W, Nick HS, Allen CM. Amplification of the *bacA* gene confers bacitracin resistance to *Escherichia coli*. J Bacteriol 1993: **175**: 3784–3789.
7. Chen YY, Clancy KA, Burne RA. *Streptococcus salivarius* urease: genetic and biochemical characterization and expression in a dental plaque *Streptococcus*. Infect Immun 1996: **64**: 585–592.
8. Cvitkovitch DG, Gutierrez JA, Behari J et al. Tn917-lac mutagenesis of *Streptococcus mutans* to identify environmentally regulated genes. FEMS Microbiol Lett 2000: **182**: 149–154.
9. Demuth DR, Lammey MS, Huck H, Lally ET, Malamud D. Comparison of *Streptococcus mutans* and *Streptococcus sanguis* receptors for human salivary agglutinin. Microb Pathog 1990: **9**: 199–211.
10. Frandsen EV, Pedrazzoli V, Kilian M. Ecology of viridans streptococci in the oral cavity and pharynx. Oral Microbiol Immunol 1991: **6**: 129–133.
11. Gerson DF. The biophysics of microbial surfactants: growth on insoluble substrates. In: Kosaric N ed. Biosurfactants, production, properties, applications. New York, NY: Marcel Dekker, Inc., 1993: 269–286.
12. Gibbons RJ, Nygaard M. Interbacterial aggregation of plaque bacteria. Arch Oral Biol 1970: **15**: 1397–1400.
13. Hamada S, Slade HD. Biology, immunology, and cariogenicity of *Streptococcus mutans*. Microbiol Rev 1980: **44**: 331–384.
14. Hamilton IA. Ecological basis for dental caries. In: Kuramitsu HK, Ellen RP, eds. Oral bacterial ecology. Wymondham, UK: Horizon Scientific Press, 2000: 219–275.
15. Klaenhammer TR. Bacteriocins of lactic acid bacteria. Biochimie 1988: **70**: 337–349.
16. Kleerebezem M, Quadri LE, Kuipers OP, de Vos WM. Quorum sensing by peptide pheromones and two-component signal transduction system in Gram-positive bacteria. Mol Microbiol 1997: **24**: 895–904.
17. Koga T, Okahashi N, Takahashi I, Kanamoto T, Asakawa H, Iwaki M. Surface hydrophobicity, adherence and aggregation of cell surface protein antigen mutants of *Streptococcus mutans* serotype c. Infect Immun 1990: **58**: 289–296.
18. Kolenbrander PE, London J. Adhere today, here tomorrow: oral bacterial adherence. J Bacteriol 1993: **175**: 3247–3252.
19. Kreth J, Merritt J, Shi W, Qi F. Competition and coexistence between *Streptococcus mutans* and *Streptococcus sanguinis* in the dental biofilm. J Bacteriol 2005: **187**: 7193–7203.
20. Kroes I, Lepp PW, Relman DA. Bacterial diversity within the human subgingival crevice. Proc Natl Acad Sci USA 1999: **96**: 14547–14552.
21. Lee MS, Morrison DA. Identification of a new regulator in *Streptococcus pneumoniae* linking quorum sensing to competence for genetic transformation. J Bacteriol 1999: **181**: 5005–5016.
22. Li YH, Lau PC, Lee JH, Ellen RP, Cvitkovitch DG. Natural genetic transformation of *Streptococcus mutans* growing in biofilms. J Bacteriol 2001: **183**: 897–908.
23. Loesche WJ. Role of *Streptococcus mutans* in human dental decay. Microbiol Rev 1986: **50**: 353–380.
24. Lucchini F, Kmet V, Cesena C, Coppi L, Bottazzi V, Morelli L. Specific detection of a probiotic *Lactobacillus* strain in faecal samples by using multiplex PCR. FEMS Microbiol Lett 1998: **158**: 273–278.
25. Matsumoto N, Salam MA, Watanabe H, Amagasa T, Senpuku H. Role of gene E2f1 in susceptibility to bacterial adherence of oral streptococci to tooth surfaces in mice. Oral Microbiol Immunol 2004: **19**: 270–276.
26. Mager DL, Ximenez-Fyvie LA, Haffajee AD, Socransky SS. Distribution of selected bacterial species on intraoral surfaces. J Clin Periodontol 2003: **30**: 644–654.
27. Millsap K, Reid G, van der Mei HC, Busscher HJ. Displacement of *Enterococcus faecalis* from hydrophobic and hydrophilic substrata by *Lactobacillus* and *Streptococcus* spp. as studied in a parallel plate flow chamber. Appl Environ Microbiol 1994: **60**: 1867–1874.
28. Motegi M, Takagi Y, Yonezawa H et al. Assessment of genes associated with *Streptococcus mutans* biofilm morphology. Appl Environ Microbiol 2006: **72**: 6277–7287.
29. Neumuller AM, Konz D, Marahiel MA. The two-component regulatory system BacRS is associated with bacitracin 'self-resistance' of *Bacillus licheniformis* ATCC 10716. Eur J Biochem 2001: **268**: 3180–3189.
30. Nyvad B, Kilian M. Microbiology of the early colonization of human enamel and root surfaces *in vivo*. Scand J Dent Res 1987: **95**: 369–380.
31. Nyvad B, Kilian M. Comparison of the initial streptococcal microflora on dental enamel in caries-active and in caries-inactive individuals. Caries Res 1990: **24**: 267–272.
32. Ohki R, Giyanto, Tateno K et al. The BceRS two-component regulatory system induces expression of the bacitracin transporter, BceAB, in *Bacillus subtilis*. Mol Microbiol 2003: **49**: 1135–1144.
33. Paster BJ, Boches SK, Galvin JL et al. Bacterial diversity in human subgingival plaque. J Bacteriol 2001: **183**: 3770–3783.
34. Peterson FC, Tao L, Scheie AA. DNA binding-uptake system: a link between cell-to-cell communication and biofilm formation. J Bacteriol 2005: **187**: 4392–4400.
35. Podlesek Z, Comino A, Herzog B et al. *Bacillus licheniformis* bacitracin-resistance ABC transporter: relationship to mammalian multidrug resistance. Mol Microbiol 1995: **16**: 969–976.
36. Rashid MH, Rumbaugh K, Passador L et al. Polyphosphate kinase is essential for biofilm development, quorum sensing, and virulence of *Pseudomonas aeruginosa*. Proc Natl Acad Sci USA 2000: **97**: 9636–9641.
37. Reichmann P, Hakenbeck R. Allelic variation in a peptide-inducible two-component system of *Streptococcus pneumoniae*. FEMS Microbiol Lett 2000: **190**: 231–236.
38. Reid G, Tieszer C. Preferential adhesion of urethral bacteria from a mixed population to a urinary catheter. Cells Mater 1993: **3**: 171–176.
39. Rickard AH, Gilbert P, High NJ, Kolenbrander PE, Handley PS. Bacterial coaggregation: an integral process in the development of multi-species biofilms. Trends Microbiol 2003: **11**: 94–100.
40. Russell MW, Mansson-Rahemtulla B. Interaction between surface protein antigen of *Streptococcus mutans* and human salivary components. Oral Microbiol Immunol 1989: **4**: 106–111.
41. Shiroza T, Kuramitsu HK. Construction of a model secretion system for oral streptococci. Infect Immun 1993: **61**: 3745–3755.
42. Sissons CH, Yakub S. Suppression of urease levels in *Streptococcus salivarius* by cysteine, related compounds and by

sulfide. Oral Microbiol Immunol 2000: **15**: 317–324.
43. Tada A, Senpuku H, Motozawa Y, Yoshihara A, Hanada N, Tanzawa H. Association between commensal bacteria and opportunistic pathogens in the dental plaque of elderly individuals. Clin Microbiol Infect 2006: **12**: 776–781.
44. Tsuda H, Yamashita Y, Shibata Y, Nakano Y, Koga T. Genes involved in bacitracin resistance in *Streptococcus mutans*. Antimicrob Agents Chemother 2002: **46**: 3756–3764.
45. Uehara Y, Kikuchi K, Nakamura T et al. Inhibition of methicillin-resistant *Staphylococcus aureus* colonization of oral cavities in newborn by viridans group streptococci. Clin Infect Dis 2001: **32**: 1399–1407.
46. Wang BY, Kuramitsu HK. Interactions between oral bacteria: inhibition of *Streptococcus mutans* bacteriocin production by *Streptococcus gordonii*. Appl Environ Microbiol 2005: **71**: 354–362.
47. Yonezawa H, Kuramitsu HK. Genetic analysis of a unique bacteriocin, Smb, produced by *Streptococcus mutans* GS5. Antimicrob Agents Chemother 2005: **49**: 541–548.
48. Yoshida A, Kuramitsu HK. Multiple Streptococcus genes are involved in biofilm formation. Appl Environ Microbiol 2002: **68**: 6283–6291.
49. Yoshida A, Ansai T, Takehara T, Kuramitsu HK. LuxS-based signaling affects *Streptococcus mutans* biofilm formation. Appl Environ Microbiol 2005: **71**: 2372–2380.

Oral Microbiology Immunology 2009: 24: 162–169
Printed in Singapore. All rights reserved

ORAL MICROBIOLOGY AND IMMUNOLOGY

Role of lysine in interaction between surface protein peptides of *Streptococcus gordonii* and agglutinin peptide

H. Koba[1,3], K. Okuda[2,3], H. Watanabe[2], J. Tagami[1,4], H. Senpuku[3]

[1]Department of Cariology and Operative Dentistry, Tokyo Medical and Dental University, Tokyo, Japan, [2]Preventive Dentistry, Graduate School, Kyushu University, Fukuoka, Japan, [3]Department of Bacteriology, National Institute of Infectious Diseases, Tokyo, Japan, [4]Center of Excellence Program for Frontier Research on Molecular, Destruction and Reconstruction of Tooth and Bone, Tokyo Medical and Dental University, Tokyo, Japan

Koba H, Okuda K, Watanabe H, Tagami J, Senpuku H. Role of lysine in interaction between surface protein peptides of Streptococcus gordonii *and agglutinin peptide. Oral Microbiol Immunol 2009: 24: 162–169.* © 2009 John Wiley & Sons A/S.

Introduction: *Streptococcus gordonii* interacts with the salivary pellicle on the tooth surface and plays an important role in dental biofilm formation. Reports show that the analog Ssp peptide (A11K; alanine to lysine at position 11 in the arranged sequence, ^{1}DYQAKLAAYQAEL^{13}) of SspA and SspB of *S. gordonii* increased binding to the salivary agglutinin (gp-340/DMBT1) peptide (scavenger receptor cysteine-rich domain 2: SRCRP2). To determine the role of lysine in the binding of the Ssp(A11K) peptide to SRCRP2, we investigated whether an additional substitution by lysine influenced the binding of Ssp(A11K) peptide to SRCRP2 using a BIAcore biosensor assay.
Methods: Six analogs of the Ssp peptide with positive charges in surface positions on the structure were synthesized using substitution at various positions.
Results: The binding activity of analog Ssp(A4K–A11K) peptide was significantly higher than the other Ssp analogs. The binding activity rose under low ionic strength conditions. The distance between positively charged amino acids in the Ssp(A4K–A11K) peptide between 4K and 11K was 1.24 ± 0.02 nm and was close to the distance (1.19 ± 0.00 nm) between Q and E, presenting a negative charged area, on SRCRP2 using chemical computing graphic analysis. The molecular angle connecting 1D–11K–4K in the Ssp(A4K–A11K) peptide secondary structure was smaller than the other peptide angles (1D–11K–XK). The Ssp(A4K–A11K) peptide showed higher inhibiting activity for *Streptococcus mutans* binding to saliva-coated hydroxyapatite than the (A11K) peptide.
Conclusion: The positioning of lysine is important for binding between Ssp peptide and SRCRP2, and the inhibiting effect on *S. mutans* binding to the tooth surface.

Key words: lysine; peptide; *Streptococcus gordonii; Streptococcus mutans;* SRCRP2

Hidenobu Senpuku, Department of Bacteriology, National Institute of Infectious Diseases, 1-23-1 Toyama, Shinjuku-ku, Tokyo 162-8640, Japan
Tel.: +81 3 5285 1111;
fax: +81 3 5285 1172;
e-mail: hsenpuku@nih.go.jp
Accepted for publication October 17, 2008

Many oral streptococci including *Streptococcus gordonii* colonize the dental plaque in large numbers and interact with the enamel salivary pellicle to form a biofilm on tooth surfaces. Early biofilm formation occurs after attachment and colonization and is dependent on both the bacterial species involved and the surface composition (4, 16, 33, 37). Mutans streptococci (*Streptococcus mutans* and *Streptococcus sobrinus*) are known to be members of the principal bacterial flora on the tooth surface and are the predominant etiological agents of human dental caries (18, 30). The mutans streptococci are able to adhere as late colonizers to the tooth surface biofilm. The adhesive capabilities of mutans streptococci and *S. gordonii* are facilitated in part by using specific surface adhesins (22, 42, 50). Because streptococcal species are isolated from the same intraoral sites and express similar surface proteins, they may compete for binding to the same array of available host receptors (2, 27, 34).

Streptococcus mutans produces surface protein adhesins, PAc (also known as AgI/II, B, P1, SpaP and MSL-1) at 190 kDa (10, 15, 23, 35, 39, 41); *S. sobrinus* produces PAg (SpaA) at 170 kDa (26, 48); and *S. gordonii* produces SspB (SspA) at 180 kDa (2, 20). These interact with salivary components including lysozyme (40, 44), soluble immunoglobulin A (31, 47), amylase (40), proline-rich proteins of 18 and 38 kDa (40), and salivary agglutinin, a 300–400 kDa protein (9). The salivary agglutinin is a member of the scavenger receptor cysteine-rich (SRCR) superfamily (21, 29). Bikker et al. synthesized consensus-based peptides from the SRCR domain and SRCR-interspersed domains and found that one peptide, the SRCR domain peptide 2 (SRCRP2) bound to *S. mutans* cells (3). Oho et al. demonstrated recombinant PAc (rPAc) bound to SRCRP2 (36). The SspB (390–T400K–402) analog peptide from the A-region of SspB was derived from *S. gordonii* and was homologous to the PAc(365–377) peptide from *S. mutans* MT8148 (43, 46) and the SspA peptide from *S. gordonii* M5 (11). SspB (390–T400K–402) peptide showed the greatest binding response to salivary components and to SRCRP2 (19); and inhibited the binding of *Streptococcus sanguinis* to salivary components by more than 50%, measured using a BIAcore assay (19). The report suggests that the region containing lysine may have binding activity to the salivary components in *S. gordonii* and *S. sanguinis*. We speculate that this peptide, in addition to inhibiting *S. gordonii* and *S. sanguinis* adhesion, may inhibit colonization by *S. mutans*.

Controlling the dental plaque bacteria is important in the prevention and treatment of oral diseases. Therefore, the development of new antimicrobial compounds effective against oral microorganisms is important in oral health research leading to oral disease prevention strategies. Recently, various types of antimicrobial peptides to oral streptococci derived from the host have been reported (1, 14, 49). Another peptide originally isolated from tree frog skin is bactericidal for *S. mutans*, *S. sobrinus*, *Actinomyces viscosus*, *Fusobacterium nucleatum*, and *Escherichia coli*. Other small peptide candidates that combat infectious disease are the tripeptides inhibiting streptococcal infections *in vivo* (38) and the P1025 peptide inhibiting *S. mutans* colonization (24). Lactoferrin peptide, Lf(480–492), inhibited rPAc binding to SRCRP2 (36). Therefore, peptides derived from various sources may have multiple functions in antimicrobial and inhibiting activities; and the effects could be beneficial to oral ecology or their application may interfere with pathogenic microorganisms. However, specificity, stability, and safety studies are required before clinical use can be considered.

Here we determined the role of the lysine residue in the surface protein peptide of *S. gordonii* as it relates to binding to salivary components. The motif sequence of SspA and SspB is -Y—L–Y—L- and is important for its α-helical secondary structure (9, 12, 19, 45). Analog peptides with substitute lysine at various amino acid positions in the peptide were constructed and used to analyse binding activities to the agglutinin peptide, SRCRP2, in BIAcore biosensor experiments. Furthermore, secondary conformations were analysed using crystallographic analyses of the various analog peptides. Adhesion of the radiolabeled reference species to saliva-coated hydroxyapatite (sHA), an *in vitro* model of the tooth surface in the mouth, was measured in the presence of the peptides to determine if the peptides inhibit binding to salivary receptors. The inhibition activities using the analog peptides in *S. mutans* binding with sHA were also studied. Understanding the role of the lysine residue in the binding peptide with SRCRP2 may lead to products to prevent dental caries in the future.

Materials and methods

Bacterial strains and culture

Streptococcus mutans MT8148 was cultured in brain–heart infusion broth (BHI, Difco Laboratory, Detroit, MI) in an aerobic atmosphere of 5% CO_2, 75% N_2, and 20% O_2 (GasPack CO_2, Becton/Deckinson, Sparks, MD) at 37°C before incubation with sHA beads.

Peptide synthesis

The amino acid sequence (DYQAKLAAYQAEL) (Table 1) was identified from streptococcal homologous expressed amino acid sequences where the -Y—L–Y—L motif is important for the α-helix secondary structure (45) in SspA and SspB derived from *S. gordonii* (11); and is homologous to the PAc(365–377, TYEAALKQYEADL) peptide from *S. mutans* MT8148 (Table 1) (19). Various peptides were constructed with substituted lysine where they expressed two or three positive charges on the peptide surface using Molecular Operating Environment (MOE) analysis (Table 2 and Fig. 1) (19). A peptide analog of the Ssp peptide was synthesized by changing the A at positions 4 and 11 to K, yielding Ssp(A4K–A11K). The PAc(316–334, YQTELARVQKANADAKATY) peptide derived from *S. mutans* (43) was used as a control for the adhesion blocking assay to sHA beads. PAc(316–334) contains two lysines but not

Table 1. Identification of universal sequence from homologous Ssp peptides

Peptide	Amino acid sequence[a]												
SspA(162-174)	E	Y	E	A	K	L	A	Q	Y	Q	K	D	L
SspA(187-199)	D	Y	Q	N	K	L	S	A	Y	Q	A	E	L
SspA(269-281)	D	Y	Q	A	K	L	A	A	Y	Q	A	E	L
SspA(326-338)	T	Y	E	A	A	L	K	Q	Y	E	A	D	L
SspA(351-363)	D	Y	Q	T	K	L	A	E	Y	Q	T	E	L
SspA(408-420)	D	Y	E	A	K	L	A	K	Y	E	A	D	L
SspB(163-175)	E	Y	E	A	K	L	A	Q	Y	Q	K	D	L
SspB(188-200)	D	Y	Q	N	K	L	S	A	Y	Q	T	E	L
SspB(270-282)	D	Y	Q	A	K	L	A	A	Y	Q	T	E	L
SspB(352-364)	D	Y	Q	A	K	L	A	A	Y	Q	T	E	L
SspB(409-421)	D	Y	E	A	K	L	A	K	Y	E	A	D	L
Consensus sequence	[1]D	Y	Q	A	K	L	A	A	Y	Q	A	E	L[13][b]

[a]Various Ssp A and Ssp B sequences were selected in previous report (11).
[b]Number indicated position in 13 mer amino acid residues.
Major amino acid in box was selected at each position as a consensus sequence.

Table 2. Amino acid sequences of Ssp peptide substituted with lysine

Peptide	Amino acid sequence
Consensus sequence	[1]DYQAKLAAYQAEL[13a]
Ssp(A11K)	DYQAKLAAYQK[b]EL
ssp(Q3K-A11K)	DYKAKLAAYQKEL
Ssp(A4K-A11K)	DYQKKLAAYQKEL
Ssp(A7K-A11K)	DYQAKLKAYQKEL
Ssp(A8K-A11K)	DYQAKLAKYQKEL
Ssp(Q10K-A11K)	DYQAKLAAYKKEL
Ssp(A4K-A11K)[2]	DYQKKLAAYQKEL–DYQKKLAAYQKEL

[a]Number indicated position in 13 mer amino acid residues.
[b]The substituted amino acid with lysine was indicated in bold.

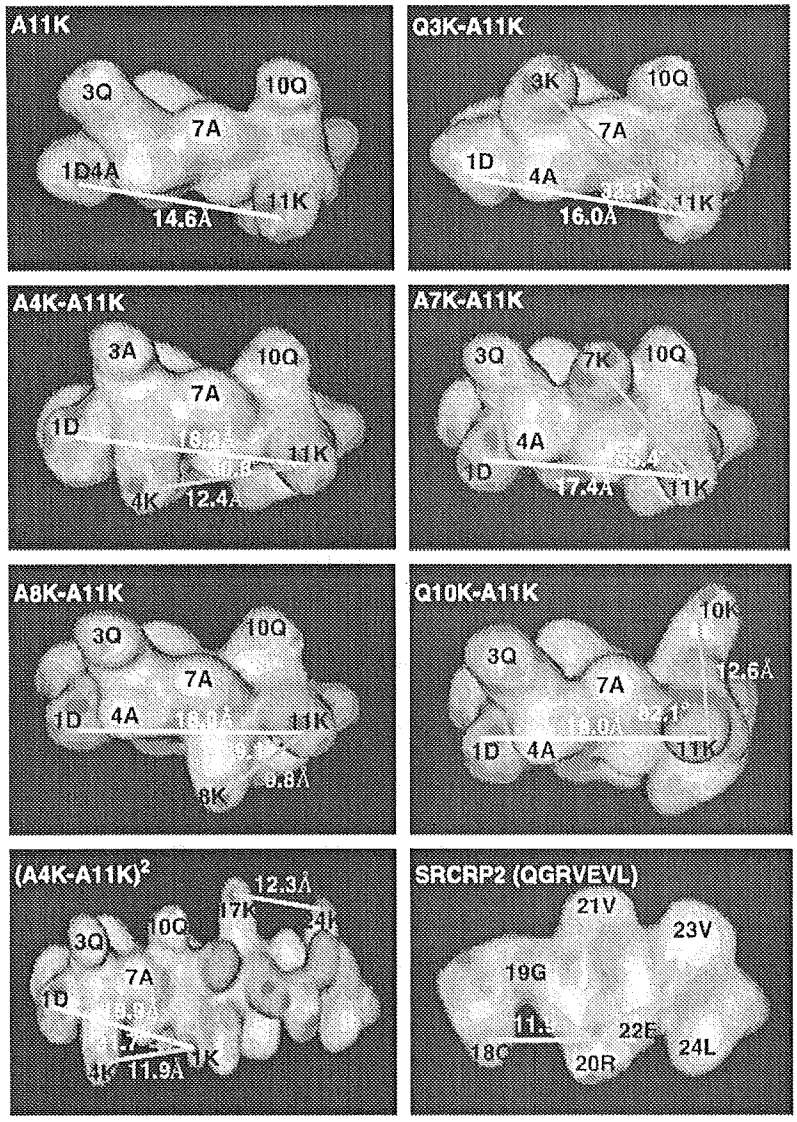

Fig. 1. Schematic representation of Ssp peptides and SRCRP2 peptides. Models of the secondary structure and surface charge (positive [blue] and negative [red]) in the peptides were constructed using MOE software with CHEMICAL COMPUTING GRAPHICS. Position numbers and the amino acid residues on the surfaces of the peptides are indicated. White and green lines indicate distances between 1D and 11K, and XK and 11K on α-helical structure in Ssp peptides. Pink line indicates a distance between 18Q and 22E on the β-sheet in SRCRP2. Arrow indicates angle between three positive charge residues.

the sequence (TYEAALKQYEADL) that is important for binding activity to salivary components. The scavenger receptor cysteine-rich domain peptide 2 (SRCRP2; QGRVEVLYRGSWGTVC) of the agglutinin/gp340/DMBT1 was used as the receptor for the synthesized bacterial peptides and was also synthesized. All peptides were synthesized using the stepwise solid-phase procedure at Scrum Inc. (Tokyo, Japan). The synthesized peptide samples were subsequently purified using reverse-phase high-performance liquid chromatography (HPLC) with a SunFire™ column (4.6 × 150 mm; Nihon Waters K.K., Tokyo, Japan) using a 5–45% acetonitrile gradient in 0.1% trifluoroacetic acid for 50 min at a flow rate of 5 ml/min. Purity was determined to be greater than 95% using HPLC. The peptides were dissolved in sterile demineralized water at 1 mg/ml; and aliquots were freeze-dried and stored at −20°C.

Modeling of the secondary structure by surface charge

Modeling of the secondary structures using the surface charges of Ssp(A11K) was performed using a MOE with the developing platform of PPh4Dock and the MMFF94s force-field subroutines, which are used for energy evaluation in this program (17). Ssp(A3K–A11K), Ssp (A4K–A11K), Ssp(A7K–A11K), Ssp(A8K–A11K), Ssp(Q10K–A11K), and doubling the synthesis peptide of Ssp(A11K) were evaluated and analysed on the basis of an α-helical structure using the MOE system (version 2006–2008, Chemical Computing Group Inc., Montreal, Quebec, Canada) (Fig. 1). An α-helical structure was constructed using a ϕ-angle of −65° and a ψ-angle of −39° with energy minimization of possible structures in these peptides; construction was performed using atom size, bond stretch, angle bend, stretch-bend, out-of-plane, torsion, and charge. Conversely, SRCRP2 is composed of two short β-sheets joined by a β-turn (3) and SRCRP2 (QGRVEVL) in a β-sheet was also constructed in MOE (Fig. 1). The distance between XK and 11K, and the angle among positive charge residues were independently analysed three times.

Immobilizing the ligand

The binding of analog peptides to SRCRP2 was determined using a BIAcore Biosensor System (BIAcore 2000, BIAcore AB, Uppsala, Sweden). We used a standard CM5 sensor chip that has a carboxymethylated

dextran-coated gold surface on the sensor chip and was activated by injecting 70 μl of a solution containing 400 mM *N*-ethyl-*N'*-(3-diethylaminoprophyl) carbodiimide and 100 mM *N*-hydroxysuccinimide at a flow rate of 10 μl/min. Following activation, 70 μl of 0.75 mg SRCRP2 peptide per milliliter in 10 mM sodium acetate buffer (pH 5.0) was applied to the chip and immobilized on its surface. Residual *N*-hydroxysuccinimide esters were then inactivated using 70 μl of 1 M ethanolamine hydrochloride. A flow rate of HBS-EP buffer saline [0.01 M HEPES pH 7.4, 0.15 M NaCl, 3 mM ethylenediaminetetraacetic acid (EDTA), 0.005% Surfactant P20] was maintained at 10 μl/min throughout the immobilization procedure. Three millimolar EDTA and 0.005% surfactant P20 were included in the buffer condition to optimize peptide binding to SRCRP2 because excess bound peptide was not completely regenerated by elution buffer and disturbed the next response in the buffer without them. Moreover, the buffer is suitable for the sensitive, stable responses recorded for the molecular binding to the receptors.

Interaction of the peptides with SRCRP2

The peptide solutions at 0.625, 1.25, and 2.5 mM in HBS-EP were exposed to the immobilized ligand on the CM5 sensor chip (flow rate, 10 μl/min); and the dissociation phase was followed by injection of HBS-EP at a rate of 10 μl/min. All binding experiments were conducted at 25°C (19, 43). At the end of each binding cycle, the surface of the sensor chip was regenerated using 50 mM glycine–NaOH (pH 9.5) for 60 s. Ssp peptide solutions at 0.625 mM were prepared with pH 4, 5, 6, and 7.4 in HBS-EP and exposed to an SRCRP2-immobilized CM5 sensor chip surface at a flow rate of 10 μl/min. Moreover, to compare the binding activities of Ssp(A4K–A11K) and Ssp(A4K–A11K)^2 (TABLE 2), peptide solutions at 0.625 mM and 1.25 mM of Ssp(A4K–A11K) and Ssp(A4K–A11K)^2 peptides were exposed to the immobilized ligand. Association (K_a) and dissociation (K_d) rate constants were analysed from the responses of all peptides to SRCRP2 using BIAEVALUATION software (BIAcore AB).

Human saliva collection

Whole saliva from five human volunteers (27–44 years old) was stimulated by chewing paraffin gum; and collected and pooled into ice-chilled sterile bottles over 5 min. The saliva was clarified by centrifugation at 10,000 *g* for 10 min at 4°C; filter sterilized; and used immediately to coat HA for the binding assays.

Inhibiting effects of the analog Ssp peptides on binding of *S. mutans* to whole saliva-coated HA

The sHA binding assay employed was originally described by Liljemark et al. (28) and Koga et al. (25), and modified for our research. We used Ssp(A11K) peptide and Ssp(A4K–A11K) peptide, which showed the highest binding activity to SRCRP2 in the BIAcore biosensor assay to assess binding inhibition of *S. mutans* MT8148 to sHA. Consensus sequence peptide and PAc(316–334) peptide, which did not show significant binding activities in the BIAcore assay, were also applied as a control for the binding inhibition assay using sHA. Twenty milligrams of HA (SANGI Co., Ltd, Tokyo, Japan) was equilibrated with phosphate-buffered saline (PBS); soaked in 1.5 ml whole saliva; incubated for 60 min at room temperature; and washed twice with sterilized PBS. Saliva-treated HA was suspended and incubated for 60 min at 37°C in 0, 0.125, 0.25, 0.375, 0.5, 0.625, and 0.75 mM of peptide solution in PBS. *Streptococcus mutans* were grown at 37°C for 18 h in BHI broth containing [methyl-^{3}H]thymidine (ICN Radiochemicals, Irvine, CA) at a final concentration of 10 μCi/ml to a specific activity of between 2.5×10^{-2} and 0.6×10^{-3} counts per min (c.p.m.)/cell. The bacteria were harvested and washed with sterilized PBS three times; suspended in PBS; sonicated on ice for 10 s; and adjusted to 5×10^7 colony-forming units in a 1.5-ml bacterial solution. The saliva-coated (sHA) specimens were suspended in the ^{3}H-labeled bacterial solution and incubated with shaking for 90 min at 37°C. Unattached cells were removed; and beads with bound ^{3}H-labeled bacteria were washed five times with sterilized PBS and transferred to a scintillation vial. After the addition of 10 ml Ultimagold Scintillation Cocktail (Packard Co., Downers Grove, IL), the radioactivity was determined using a liquid scintillation counter (LSC-5000, Aloka Co. Ltd., Tokyo Japan). Unattached cells were also pooled and their radioactivity was determined. In the input of 7.5×10^7 cells, 60% of cells attached to the sHA and showed radioactivity ranging from 36,500 to 42,500 c.p.m. in the assay without the peptide. Background values were less than 100 c.p.m.

Statistical analysis

Statistical analysis was performed using the Mann–Whitney's *U*-test. Differences at the 0.05 level or less were considered to be statistically significant.

Results

Identification of the native amino acid sequence

The consensus amino acid sequence was studied in 11 streptococcal homologous sequences of SspA and SspB to PAc(365–377) (Table 1). The 13 amino acid residues were re-aligned from No. 1 to No. 13. Position 1 showed a negatively charged amino acid, a D in six sequences, and neutral and negative amino acids (E and Q) and T in the other four sequences where D was selected as a major amino acid at position 1. Position 3 showed Q in six sequences and E in five sequences where Q was selected as a major amino acid at position 3. In the same way, amino acids at all positions were selected to yield the consensus sequence: (^{1}DYQAKLAAYQ-AEL^{13}) (Table 1). The sequence differed at position 400 in amino acid residue from SspB(390–402) (DYQAKLAAYQTEL) as previously reported (9). The analog substituted from A to K at position 11 (A11K) was identical with the SspB(390–T400K–402), which was previously reported as the highest binding peptide to SRCRP2 using the BIAcore assay (19). Therefore, we considered that the Ssp(A11K) peptide was a universal binding analog peptide of SspA and SspB to the salivary agglutinin, SRCRP2.

Binding of the Ssp peptides to SRCRP2

To determine the role of lysine in the binding of Ssp(A11K) peptide to SRCRP2, we investigated whether additional substitutions of lysine influenced the binding of the Ssp(A11K) peptide to SRCRP2. Each peptide (0.625, 1.25, and 2.5 mM) was applied to the sensor chip after it was immobilized with SRCRP2. K_a and K_d were observed using BIAEVALUATION software (Fig. 2). The K_a ($7.6 \pm 1.1 \times e^3$) of Ssp(A4K–A11K) peptide to the immobilized SRCRP2 on the sensor-chip was significantly higher than that of the Ssp(A11K) peptides ($3.1 \pm 1.2 \times e^3$) (Fig. 2). Ssp(A4K–A11K) peptide showed dose-dependent binding activities (data not shown). In other lysine-substituted peptides, the K_a ($2.2 \pm 0.6 \times e^3$, $6.8 \pm 4.5 \times e^3$, and $3.8 \pm 1.9 \times e^3$) of Ssp(Q3K–A11), Ssp(A7K–A11K), and Ssp(A8K–

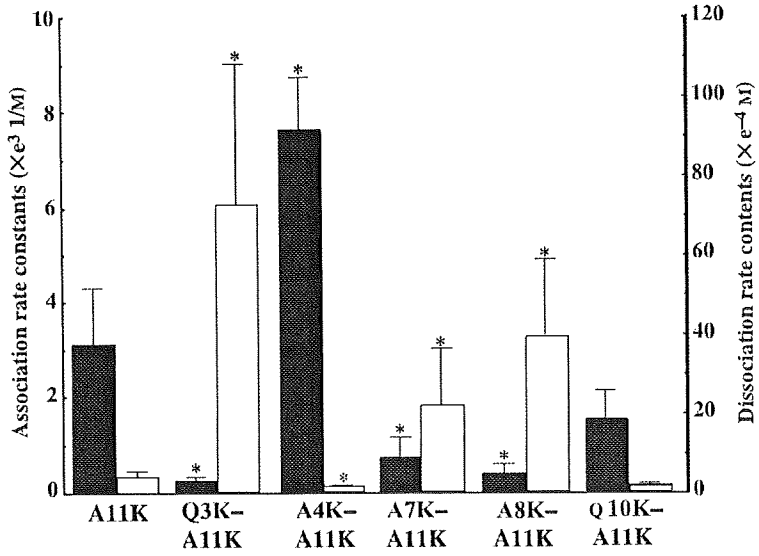

Fig. 2. Binding of various Ssp peptides to immobilized SRCRP2. The peptide solutions (0.625, 1.25, and 2.5 mM) were exposed to the immobilized CM5 sensor chip with SRCRP2 in HBS-EP pH 7.4. The association (K_a, ■) and dissociation (K_d, □) rate constants were analysed using BIAEVALUATION software. The results were expressed as mean ± standard deviation for four independent assays. The asterisks indicate significant difference as follows: one asterisk, $P < 0.01$ compared with the Ssp(A11K) peptide.

A11K) peptide, respectively, were significantly lower than that of Ssp(A11K) peptide (Fig. 2). For the K_d, the inverse relationship of responses between lysine-substituted peptide and Ssp(A11K) compared with K_a was observed (Fig. 2). Control peptide, PAc(316–334) peptide and consensus sequence peptide did not show significant binding activity, and K_a and K_d were not analysed. Moreover, Ssp(A4K–A11K) peptide showed a higher K_a at a low pH than Ssp(A11K) and Ssp(A8K–A11K) peptides (Table 3). Ssp(A8K–A11K) peptide showed a lower K_a than Ssp(A11K) peptide at only pH 6.0 in the buffer. To determine the mechanisms of Ssp(A4K–A11K) peptide binding to SRCRP2, the binding activity of synthetic double peptide Ssp(A4K–A11K)^2 was compared with that of the single peptide of Ssp(A4K–A11K). The K_a ($6.6 \pm 3.0 \times e^{3}$) and K_d ($1.9 \pm 0.8 \times e^{-4}$) binding activities of Ssp(A4K–A11K)^2 peptide were similar to those ($6.9 \pm 3.2 \times e^{3}$ and $1.7 \pm 0.9 \times e^{-4}$, respectively) of Ssp (A4K–A11K) peptide. Therefore, the binding between Ssp(A4K–A11K) and SRCRP2 may be dependent on the single interaction receptor and ligand, and on molecular size.

Secondary structure and surface charge

To assess the binding shape of the molecule of the analog peptides to SRCRP2, their secondary structures and surface charges were visually analysed using chemical computing analysis with MOE (Fig. 1). Ssp(A4K–A11K) peptide had the highest binding activity to SRCRP2 (Fig. 2) and showed three surface positive charge areas at residues 1(D), 4(K), and 11(K). The distance between XK and 11K, and angles of 1D–11K–XK in these peptides are shown in Table 3. The distance between 4K and 11K was 1.24 ± 0.02 nm close to the distance (1.19 ± 0.00 nm) between the amino acids (Q and E) presenting a negative charge area in the β-sheet of SRCRP2 (Fig. 1; Table 4). Aspartic acid is not positively charged; however, a surface positive charge area at position 1 of Ssp(A4K–A11K) peptide is partially shown in the crystallographic analysis (Fig. 1) (19). This suggests that the main chain (amidohydrogen) in D is expressed on the surface of the α-helical peptide structure at N-terminal head. The angle among three positive charged residues of 1D–11K–4K was 30.8 ± 4.4° and was smaller than in the Ssp(A7K–A11K), Asp(A8K–A11K) and Ssp(Q10K–A11K) peptides (Fig. 1; Table 4). The angle was similar in the Ssp(Q3K–A11K) peptide and Ssp(A4K–A11K); but the distance between the 3K and 11K was longer in Ssp(Q3K–A11K) than in the Ssp(A4K–A11K) peptide. The expressive direction of the positive charge area at 1D in Ssp(Q3K–A11K) peptide differed from that in the Ssp(A4K–A11K) peptide (Fig. 1). In contrast, the Ssp(Q10K–A11K) peptide showed a close distance between the amino acids presenting a positive charge area compared with between the amino acids presenting a negative charge area on the β-sheet in SRCRP2; but the angle of 1D–11K–10K was higher than those in the other peptides (Table 4). The Ssp(A7K–A11K) and Ssp(A8K–A11K) peptides showed a lower distance in XK–11K than 4K–11K in Ssp(A4K–A11K). The (A4K–A11K)^2 peptide showed a similar distance in XK–11K compared with the Ssp(A4K–A11K) peptide; but the angle of 1D–XK–11K was higher than that of the Ssp(A4K–A11K) peptide.

Effects of Ssp analog peptide on sHA

To observe whether the binding ability of Ssp(A4K–A11K) peptide affected *S. mutans* binding to sHA, a binding assay

Table 3. Association (Ka) and dissociation (Kd) rate constants of three peptides against SRCRP2

	Ka (l/M)			Kd (M)		
	A11K	A4K-A11K	A8K-A11K	A11K	A4K-A11K	A8K-A11K
pH4	$3.9 \pm 1.9 \times e^{3}$	$9.7 \pm 2.5 \times e^{3}$*	$4.1 \pm 1.0 \times e^{3}$	$3.1 \pm 1.3 \times e^{-4}$	$1.1 \pm 0.3 \times e^{-4}$*	$2.6 \pm 0.8 \times e^{-4}$
pH5	$4.6 \pm 1.8 \times e^{3}$	$9.5 \pm 2.1 \times e^{3}$*	$4.5 \pm 1.4 \times e^{3}$	$2.5 \pm 1.1 \times e^{-4}$	$1.1 \pm 0.3 \times e^{-4}$*	$2.2 \pm 0.6 \times e^{-4}$
pH6	$1.7 \pm 0.9 \times e^{3}$	$6.4 \pm 2.3 \times e^{3}$*	$6.5 \pm 4.8 \times e^{2}$**	$8.3 \pm 6.3 \times e^{-4}$	$1.8 \pm 1.0 \times e^{-4}$**	$2.5 \pm 2.1 \times e^{-3}$**
pH7.4	–	$1.4 \pm 0.9 \times e^{-4}$	–	–	$1.3 \pm 1.2 \times e^{-3}$	–

The peptide solutions (0.625 mM) were applied to the immobilized CM5 sensor chip with SRCRP2 in HBS-EP pH4, 5, 6 and 7.4. Ka and Kd were analysed by BIAEVALUATION software. The results are expressed as mean ± SD for six independent assays. The asterisks indicate significant difference as follows: one and two asterisks, $P < 0.01$ and $P < 0.05$ compared the Ssp(A11K) peptide in 4, 5, 6 or 7.4 pH condition.
–, Data were not analysed because of low value in BIAcore.

Table 4. Substituted Ssp peptides' analysis utilizing MOE

Ssp peptide	Distance (Å) between positive charges 1D-11K	Distance (Å) between positive charges on lysine XK-11K		Angle (°) among positive charge 1D-11K-XK	
A11K	14.6 ± 0.3				
Q3K-A11K	16.0 ± 0.3	3K-11K	14.1 ± 0.2	1D-11K-3K	33.1 ± 3.6
A4K-A11K	18.3 ± 0.6	4K-11K	12.1 ± 0.2	1D-11K-4K	30.8 ± 4.4
A7K-A11K	17.4 ± 0.5	7K-11K	10.1 ± 0.2	1D-11K-7K	55.4 ± 0.8
A8K-A11K	18.0 ± 0.9	8K-11K	9.8 ± 0.5	1D-11K-8K	39.1 ± 0.5
Q10K-A11K	18.0 ± 0.8	10K-11K	12.6 ± 0.0	1D-11K-10K	82.1 ± 0.0
$(A4K-A11K)^2$	19.9 ± 0.8	4K-11K	16.9 ± 0.4	1D-11K-4K	31.7 ± 5.0

The results were analysed in chemical computing graphic (Fig. 1) and expressed as mean ± SD for three times analysis.

of *S. mutans* using saliva-coated HA beads was performed. Cell adherence by *S. mutans* was significantly inhibited by pretreatment with 0.625 mM Ssp(A11K) peptide on the sHA but not by pretreatments with less than 0.625 mM of the peptide (Fig. 3). The binding was also inhibited by pretreatment using the Ssp(A4K–A11K) peptide at 0.5, 0.625, and 0.75 mM (Fig. 3). However, the consensus sequence peptide and control peptide, PAc(316–334), did not show a significant inhibition in application of peptide at 0.625 mM (Fig. 3). This suggests the Ssp(A4K–A11K) peptide has a higher inhibition activity in binding *S. mutans* to sHA than the Ssp(A11K) peptide.

Discussion

In the N-terminal region (residues 1–429) of *S. gordonii* M5 cells, the surface adhesins, SspB and SspA, are 96% identical and show homology with SpaP (PAc) at 63% and 60% identity, respectively (10). The A-region is composed of three long and two incomplete repeating sequences (33). Therefore, it is considered that the some sequences that are homologous to the amino acid sequence ^{365}TYEAAL-KQYEADL^{377} of PAc(365–377) (43, 45) exist in SspA and SspB. In the present study, the consensus sequence was found by arrangement and might be an important sequence for the initial attachment of *S. gordonii* to the tooth surface. The sequence includes only one lysine, at position 5 where its binding activity is weak. However, the analog, Ssp(A11K) peptide, has a substitute A to K at position 11 in the native protein and shows the highest binding to the salivary components and SRCRP2 (19); it may also have an inhibiting effect on competing with colonizers such as *S. gordonii*, *S. sanguinis*, and *S. mutans*. Here we observed the inhibiting effects of Ssp(A11K) peptide in the binding assay of *S. mutans* to sHA (Fig. 3). The inhibiting effects were also observed in the binding assay of *S. gordonii* but not that of *Streptococcus mitis* (data not shown). *Streptococcus gordonii* may compete with *S. mutans* but not *S. mitis* for salivary adhesion sites such as the homologous SspA and SspB regions and PAc(365–377). Additional substitution by lysine at position 4 in Ssp(A11K) peptide elevated the binding and bacterial inhibiting activities of the Ssp(A11K) peptide. Furthermore, the binding activity rose at low ionic strength using the BIAcore assay (Fig. 3). The data suggest that the presence of an additional positive surface charge by substituting two lysines may have an important role in the binding of the peptide and may lead to stronger inhibition of bacteria to the tooth surface. Additionally, the data demonstrate that of the three cationic lysine residues, only the residues Lys-4 and Lys-11 contribute to the binding to SRCRP2. Further analysis shows that Lys-4 in the α-helical structure makes a significant contribution to the surface positive potential of the peptide.

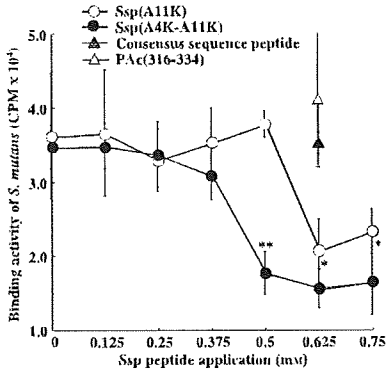

Fig. 3. Inhibition by Ssp peptides of *Streptococcus mutans* adherence on saliva-coated hydroxyapatitie (sHA). The adherence levels (counts per minute) of *S. mutans* MT8148 to sHA treated with 0, 0.125, 0.375, 0.5, 0.625, and 0.75 mM of Ssp(A11K) and Ssp(A4K–A11K) peptides, respectively, are shown. Treatments with 0.625 mM, consensus sequence peptide and PAc(316–334) peptide were performed as controls. The results are expressed as mean ± SD for three independent assays.

The physical interaction of these cationic peptides to anionic interfaces was previously investigated for other antimicrobiological agents (5, 6, 8, 32). Many naturally occurring antimicrobial peptides consist of linear molecules with the potential to adopt an amphipathic α-helical confirmation and interact with lipid bilayers in membranes (13, 51). Davies et al. reported that the α-helical structure region containing three lysine residues in a linear fatty acid-binding protein interacted with the anionic interface as a result of initial electrostatic interaction (8). Only those cationic residues contribute significantly to this binding. Other investigators suggest that apoliprotein A-I lysine positive charges play an important role in the specific recognition of negatively charged phospholipids on the surface of an ABCA1 (5). These results support our data that the positively charged amino acid residue, i.e. lysine, is essential for binding activity on the peptide surface, the positively charged α-helical structure, to the negatively charged interface on SRCRP2.

Cheng et al. suggest that ion-pairing (lysine and negative charged functional groups) interactions are important for protein stabilization (7). The C-terminal neighbor of lysine at position 4 and 11 was Q, having a negatively charged amino acid at positions 3 and 10 in the Ssp(A4K–A11K) peptide (Table 2). Other substituted peptides did not show such ion-pairing in addition to Q and K at position 10 and 11. Therefore, it is considered that the substitutions of two lysines, which induce a significant binding activity to SRCRP2, form durable interactions with the negatively charged amino acid; Q. The stability may influence the inhibition activity of *S. mutans* binding to sHA.

The differences in the secondary structure between Ssp(A4K–A11K) peptide and other analogous peptides were visualized on the basis of the α-helical structure; and the surface charges were plotted using chemical computing graphics (Fig. 1). The binding activity may be associated with the molecular distance between surface positive charges in the α-helical structure and may be close to the distance between the amino acids presenting surface negative charges in the SRCRP2 β-sheet. In contrast, the K_a of Ssp(Q3K–A11K), Ssp(A7K–A11K), and Ssp(A8KA11K) peptides (which were observed to have different distances between the positive charges and between the negative charges from SRCRP2), were lower than those of

Ssp(A4K–A11K) and Ssp(A11K) peptides (Table 3). Therefore, double lysine-substituted Ssp peptides excepting Ssp(A4K–A11K) might change the conformation of the Ssp(A11K) peptide, which was required for binding activity. The expressive directions of some of the positive charges in the Ssp(A4K–A11K) peptide were different from the other peptides (Fig. 1). The angle connecting the three positively charged residues (1D–11K–4K) in the Ssp(A4K–A11K) peptide was smaller than the other peptide angles (1D–11K–XK) (Fig. 1; Table 3). These results indicated the peptide-positioning amino acid with a positive charge, the distance between positively charged residues, the expressive direction of the positive charge, and the linear-like connection with the positively charged residues on the α-helical confirmation may be necessary for the inhibition of *S. mutans* adherence on the tooth surface.

Competitive binding of Ssp(A4K–A11K) peptide is strongly suggested to occur through interactions with a salivary pellicle constituent(s) and the adhesion to sHA is maintained even in the presence of a competing peptide. We speculate that the Ssp(A4K–A11K) peptide binds to SRCRP2 and interferes with the attachment of *S. mutans* to the salivary components. Another possibility that cannot be ruled out is that the Ssp(A4K–A11K) peptide inhibits binding of *S. mutans* to other salivary receptors. The binding of fluorescein isothiocyanate-labeled peptide to the sHA can be visualized using a microscope (data not shown) and the inhibiting level of Ssp(A4K–A11K) peptide was about 50%. In other reports, anti-PAc(365–377) antibodies and monoclonal antibody from mice immunized with PAc(365–377) peptide show 47.2% and 56.6% binding inhibition to salivary components and tooth surface in rats (43, 46). The homologous region to PAc(365–377) in SspA/B and PAc might not contribute completely to the binding of *S. gordonii* and *S. mutans* to salivary components. Taken together, the inhibition by Ssp (A4K–A11K) peptide may be restricted by the potential of interactions between SspA/B and salivary receptors and the affinity levels of peptides to the salivary receptors.

Our data suggest that the binding to salivary agglutinin and the specific inhibition of *S. mutans* adherence required the positioning of a positive charge on lysine at positions 4 and 11 in the Ssp consensus sequence and three surface positive charge connections on α-helical structure. The Ssp(A4K–A11K) peptide may be employed as an antiadherence peptide in future therapy of oral infections. It may, therefore, be useful for the prevention of dental caries in clinical treatments.

Acknowledgments

This work was supported in part by a grant-in aid for the Development Scientific Research (19659559) from the Ministry of Education, Science, and Culture of Japan, and by a grant from the Ministry of Health, Labor and Welfare (H19-Medical Services-007).

References

1. Altman H, Steinberg D, Porat Y et al. In vitro assessment of antimicrobial peptides as potential agents against several oral bacteria. J Antimicrob Chemother 2006: **58**: 198–201.
2. Appelbaum B, Golub E, Holt SC, Rosan B. In vitro studies of dental plaque formation: adsorption of oral streptococci to hydroxyaptite. Infect Immun 1979: **25**: 717–728.
3. Bikker FJ, Ligtenberg AJ, Nazmi K et al. Identification of the bacteria-binding peptide domain on salivary agglutinin (gp-340/DMBT1), a member of the scavenger receptor cysteine-rich superfamily. J Biol Chem 2002: **277**: 32109–32115.
4. Bowden GH. Microbiology of root surface caries in humans. J Dent Res 1990: **69**: 1205–1210.
5. Brubaker G, Peng DQ, Somerlot B, Abdollahian DJ, Smith JD. Apolipoprotein A-I lysine modification: effects on helical content, lipid binding and cholesterol acceptor activity. Biochim Biophys Acta 2006: **1761**: 64–72.
6. Buckland AG, Wilton DC. Anionic phospholipids, interfacial binding and the regulation of cell functions. Biochim Biophys Acta 2000: **1483**: 199–216.
7. Cheng RP, Girinath P, Ahmad R. Effect of lysine side chain length on intra-helical glutamate–lysine ion pairing interactions. Biochemistry 2007: **46**: 10528–10537.
8. Davies JK, Hagan RM, Wilton DC. Effect of charge reversal mutations on the ligand- and membrane-binding properties of liver fatty acid-binding protein. J Biol Chem 2002: **277**: 48395–48402.
9. Demuth DR, Golub EE, Malamud D. Streptococcal–host interactions. Structural and functional analysis of a *Streptococcus sanguis* receptor for a human salivary glycoprotein. J Biol Chem 1990: **265**: 7120–7126.
10. Demuth DR, Lammey MS, Huck M, Lally ET, Malamud D. Comparison of *Streptococcus mutans* and *Streptococcus sanguis* receptors for human salivary agglutinin. Microb Pathog 1990: **9**: 199–211.
11. Demuth DR, Duan Y, Brooks W, Holmes AR, McNab R, Jenkinson HF. Tandem genes encode cell-surface polypeptides SspA and SspB which mediate the adhesion of the oral bacterium *Streptococcus gordonii* to human and bacterial receptors. Mol Microbiol 1996: **20**: 403–413.
12. Demuth DR, Irvine DC. Structural and functional variation within the alanine-rich repetitive domain of streptococcal antigen I/II. Infect Immun 2002: **70**: 6389–6398.
13. Dathe M, Wieprecht T. Structural features of helical antimicrobial peptides: their potential to modulate activity on model membranes and biological cells. Biochim Biophys Acta 1999: **1462**: 71–87.
14. Drobni M, Li T, Kruger C et al. Host-derived pentapeptide affecting adhesion, proliferation, and local pH in biofilm communities composed of *Streptococcus* and *Actinomyces* species. Infect Immun 2006: **74**: 6293–6299.
15. Forester H, Hunter N, Knox KW. Characteristics of a high molecular weight extracellular protein of *Streptococcus mutans*. J Gen Microbiol 1983: **129**: 2779–2788.
16. Hajishengallis G, Koga T, Russell MW. Affinity and specificity of the interactions between *Streptococcus mutans* antigen I/II and salivary components. J Dent Res 1994: **73**: 1493–1502.
17. Halgren TA. Merck Molecular force field. J Comput Chem 1996: **17**: 490–519.
18. Hamada S, Slade HD. Biology, immunology, and cariogenicity of *Streptococcus mutans*. Microbiol Rev 1980: **44**: 331–384.
19. Hamada T, Kawashima M, Watanabe H, Tagami J, Senpuku H. Molecular interactions of surface protein peptides of *Streptococcus gordonii* with human salivary components. Infect Immun 2004: **72**: 4819–4826.
20. Holmes AR, Gelbert C, Wells JM, Jenkinson HF. Binding properties of *Streptococcus gordonii* SspA and SspB (antigen I/II family) polypeptides expressed on the cell surface of *Lactococcus lactis* MG1363. Infect Immun 1998: **66**: 4633–4639.
21. Holmskov U, Lawson P, Teisner B et al. Isolation and characterization of a new member of the scavenger receptor superfamily, glycoprotein-340(gp-340), as a lung surfactant protein-D binding molecule. J Biol Chem 1997: **272**: 13743–13749.
22. Jenkinson HF, Lamont RJ. Streptococcal adhesion and colonization. Crit Rev Oral Biol Med 1997: **8**: 175–200.
23. Kelly C, Evans P, Bergmeier L et al. Sequence analysis of the cloned streptococcal cell surface antigen I/II. FEBS Lett 1989: **258**: 127–132.
24. Kelly CG, Younson JS, Hikmat BY et al. A synthetic peptide adhesion epitope as a novel antimicrobial agent. Nat Biotechnol 1999: **17**: 42–47.
25. Koga T, Okahashi N, Takahashi I, Kanamoto T, Asakawa H, Iwaki M. Surface hydrophobicity, adherence, and aggregation of cell surface protein antigen mutants of *Streptococcus mutans* serotype c. Infect Immun 1990: **58**: 289–296.
26. LaPolla RJ, Haron JA, Kelly CG et al. Sequence and structural analysis of surface protein antigen I/II (SpaA) of *Streptococcus sobrinus*. Infect Immun 1991: **59**: 2677–2685.
27. Liljemark WF, Schauer SV. Competitive binding among oral streptococci to

hydroxyapatite. J Dent Res 1977: **56**: 157–165.
28. Liljemark WF, Bloomquist CG, Germaine GR. Effect of bacterial aggregation on the adherence of oral streptococci to hydroxyapatite. Infect Immun 1981: **31**: 935–941.
29. Ligtenberg TJ, Bikker FJ, Groenink J et al. Human salivary agglutinin binds to lung surfactant protein-D and is identical with scavenger receptor protein gp-340. Biochem J 2001: **359**: 243–248.
30. Loesche WJ. Role of *Streptococcus mutans* in human dental decay. Microbiol Rev 1986: **50**: 353–380.
31. Loimaranta V, Jakubovics NS, Hytonen J, Finne J, Jenkinson HF, Stromberg N. Fluid- or surface-phase human salivary scavenger protein gp340 exposes different bacterial recognition properties. Infect Immun 2005: **73**: 2245–2252.
32. Maloy WL, Kari UP. Structure–activity studies on megainins and other host defense peptide. Biopolymers 1995: **37**: 105–122.
33. McEldowney S, Fletcher M. Adhesion of bacteria from mixed cell suspension to solid surfaces. Arch Microbiol 1987: **148**: 57–62.
34. Nobbs AH, Zhang Y, Khammanivong A, Herzberg MC. *Streptococcus gordonii* Hsa environmentally constrains competitive binding by *Streptococcus sanguinis* to saliva-coated hydroxyapatite. J Bacteriol 2007: **189**: 3106–3114.
35. Okahashi N, Sasakawa C, Yoshikawa CM, Hamada S, Koga T. Cloning of a surface protein antigen gene from serotype c *Streptococcus mutans*. Mol Microbiol 1989: **3**: 221–228.
36. Oho T, Bikker FJ, NieuwAmerongen AV, Groenink J. A peptide domain of bovine milk lactoferrin inhibits the interaction between streptococcal surface protein antigen and a salivary agglutinin peptide domain. Infect Immun 2004: **72**: 6181–6184.
37. Pratt-Terpstra IH, Weerkamp AH, Busscher HJ. The effects of pellicle formation on streptococcal adhesion to human enamel and artificial substrata with various surface free-energies. J Dent Res 1989: **68**: 463–467.
38. Bjorck L, Akesson P, Buhus M et al. Bacterial growth blocked by a synthetic peptide based on the structure of a human proteinase inhibitor. Nature 1989: **337**: 385–386.
39. Russell MW, Lehner T. Characterisation of antigens extracted from cells and culture fluids of *Streptococcus mutans* serotype c. Arch Oral Biol 1978: **23**: 7–15.
40. Russell MW, Mansson-Rahemtulla B. Interaction between surface protein antigens of *Streptococcus mutans* and human salivary components. Oral Microbiol Immunol 1989: **4**: 106–111.
41. Russell RR. Wall-associated protein antigens of *Streptococcus mutans*. J Gen Microbiol 1979: **114**: 109–115.
42. Scannapieco FA. Saliva–bacterium interactions in oral microbial ecology. Crit Rev Oral Biol Med 1994: **5**: 203–248.
43. Senpuku H, Miyauchi T, Hanada N, Nisizawa N. An antigenic peptide inducing cross-reacting antibodies inhibiting the interaction of *Streptococcus mutans* PAc with human salivary components. Infect Immun 1995: **63**: 4695–4703.
44. Senpuku H, Kato H, Todoroki M, Hanada N, Nisizawa T. Interaction of lysozyme with a surface protein antigen of *Streptococcus mutans*. FEMS Microbiol Lett 1996: **139**: 195–201.
45. Senpuku H, Kato H, Takeuchi H, Noda A, Nisizawa T. Identification of core B cell epitope in the synthetic peptide inducing cross-inhibiting antibodies to a surface protein antigen of *Streptococcus mutans*. Immunol Invest 1997: **26**: 531–548.
46. Senpuku H, Matin K, Abdus SM et al. Inhibitory effects of MoAbs against a surface protein antigen in real-time adherence in vitro and recolonization in vivo of *Streptococcus mutans*. Scand J Immunol 2001: **54**: 109–116.
47. Takamatsu D, Bensing BA, Prakobphol A, Fisher SJ, Sullam PM. Binding of the streptococcal surface glycoproteins GspB and Hsa to human salivary proteins. Infect Immun 2006: **74**: 1933–1940.
48. Tokuda M, Okahashi N, Takahashi I et al. Complete nucleotide sequence of the gene for a surface protein antigen of *Streptococcus sobrinus*. Infect Immun 1991: **59**: 3309–3312.
49. Wei GX, Campagna AN, Bobek LA. Effect of MUC7 peptide on the growth of bacteria and on *Streptococcus mutans* biofilm. J Antimicrob Chemother 2006: **57**: 1100–1109.
50. Whittaker CJ, Klier CM, Kolenbrander PE. Mechanisms of adhesion by oral bacteria. Annu Rev Microbiol 1996: **50**: 513–552.
51. Wieprecht T, Apostolov O, Beyermann M, Seeling J. Thermodynamics of the alpha-helix-coil transition of amphipathic peptides in a membrane environment: implications for the peptide-membrane binding equilibrium. J Mol Biol 1999: **294**: 785–794.

Jpn. J. Infect. Dis., 62, 337-342, 2009

Original Article

Effects of IgY against *Candida albicans* and *Candida* spp. Adherence and Biofilm Formation

Taisuke Fujibayashi[1,4], Moriyuki Nakamura[1,4], Akira Tominaga[2,4], Norifumi Satoh[3], Taketo Kawarai[4], Naoki Narisawa[4], Osamu Shinozuka[1], Haruo Watanabe[4], Tsuneyoshi Yamazaki[1], and Hidenobu Senpuku[4]*

[1]*Dentistry for Persons with Disabilities, Tokyo Medical and Dental University, Tokyo 113-8510;*
[2]*Oral Surgery, Tokyo Medical University, Tokyo 160-0023;*
[3]*EN Otsuka Pharmaceutical Co. Ltd R&D Laboratories, Tokyo 101-0062; and*
[4]*Department of Bacteriology I, National Institute of Infectious Diseases, Tokyo 162-8640, Japan*

(Received February 4, 2009. Accepted June 22, 2009)

SUMMARY: The fungal pathogen *Candida albicans* is an opportunistic fungal pathogen that causes oral and vaginal mucosal infections as well as systemic disease. The ability of *C. albicans* to adhere to host surfaces is positively correlated with its pathogenicity. We prepared a polyclonal anti-*Candida albicans* antibody in chicken egg yolk (anti-*C. albicans* IgY) and investigated its in vitro effectiveness in preventing *C. albicans* adherence and biofilm formation. Anti-*C. albicans* IgY significantly reduced the adherence of *C. albicans* SC5314 to human oral epithelial cells in a dose-dependent manner. The same effect was also observed in other *Candida* spp. including *C. albicans* serotype A and B. Further, the IgY inhibited biofilm formation of *C. albicans* in medium without serum, but the inhibition was slightly restored in medium conditioned with 10% serum. The data indicate that anti-*C. albicans* IgY cross-reacted with various *Candida* spp. and may have a protective effect against oral candidiasis and reduce the dissemination of *Candida* spp. This effect may be due to the blocking of the binding of *Candida* spp. to the host cells. However, the blocking did not play a role when *Candida* formed a germ tube in the presence of serum. Therefore, anti-*C. albicans* IgY may be considered as a prophylactic immunotherapy or possibly an adjunctive antifungal therapy under limited conditions.

INTRODUCTION

Most bacteria and fungi that exist in humans as surface-attached communities are called biofilms, and such communities usually affect human health. The tissues are the substrates for the formation of biofilms, and the microorganisms in the biofilms serve as reservoirs to continuously seed an infection. The fungal pathogen *Candida albicans* is an opportunistic fungal pathogen that causes oral and vaginal mucosal infections as well as systemic disease (1). The ability of *C. albicans* to adhere to host surfaces is positively correlated with its pathogenicity (2). It produces adherent biofilms on a variety of different surfaces in vitro (3-6). Biofilm formation begins with surface adherence of the yeast form, which grows to yield a basal layer. The basal layer cells include some hyphae, or long tubular chains of cells, which extend to yield an upper layer that is almost exclusively hyphae. As the biofilm matures, it produces an extracellular matrix containing predominantly carbohydrate and protein (7-9).

Adherence is a critical property for biofilm microbial cells, with multiple adhesion molecules functioning in successful biofilm formation. Specific adherence to the protein surface is provided by several surface adhesins of *Candida*. Recent reports have demonstrated that antibodies with defined specificities to these surface adhesins show different degrees of protection against systemic and mucosal candidiasis (10-12). Secretory immunoglobulin A (sIgA) is thought to play a central role by inhibiting *Candida* adherence to host cells (13-15). Complex mixtures of antibodies having different specificities such as those found in salivary sIgA are shown to decrease adhesion of *C. albicans* to the host surface but do not inhibit germination (16). Therefore, the use of antibodies as an adjunct to antifungal drugs may be considered one approach to protecting against candidiasis.

Chicken eggs are known as an inexpensive and convenient source for mass production of specific antibodies (17). Specific egg yolk immunoglobulin (IgY) can be produced in egg yolk by immunizing hens with specific antigens. IgY is isolated in large quantities from the yolk by simple methods without distress to the birds (18), and has been used extensively for the treatment and prevention of various infections in animals and humans with mixed success (19-26). In particular, polyclonal anti-*C. albicans* antibody in chicken egg yolk prevented *C. albicans* from adhering to oral epithelial cells where the effect depended on the density of the infection (27). However, the IgY was induced by immunization with the *C. albicans* yeast form and included antibodies against various antigens. In general, the activity and diversity of IgY against *Candida* spp. are not well understood. The objective of this study was to evaluate the efficacy of a specific IgY against *C. albicans* and other *Candida* strains to develop an alternative therapy for candidiasis.

MATERIALS AND METHODS

Yeast strains: *C. albicans* SC5314 (serotype A), NIH207 (serotype A) and NIH792 (serotype B), *Candida tropicalis* IFO0618, *Candida dubliniensis* CD36 and CD57, *Candida parapsilosis* ATCC22019 and FRCP-0201, *Candida glabrata*

*Corresponding author: Mailing address: Department of Bacteriology I, National Institute of Infectious Diseases, 1-23-1 Toyama, Shinjuku-ku, Tokyo 162-8640, Japan. Tel: +81-3-5285-1111, Fax: +81-3-5285-1163, E-mail: hsenpuku@nih.go.jp

850821 and CBS138 were used. All strains were provided by Dr. Masakazu Niimi from the National Institute of Infectious Diseases. For use in experiments, all organisms were grown in liquid Yeast Peptone Dextrose (YPD; 2% Bacto peptone, 2% dextrose and 1% Yeast extract) broth aerobically at 37°C; and washed three times in phosphate-buffered saline (PBS). Then they were suspended to the appropriate concentration in PBS.

Preparation of IgY: Anti-*C. albicans* IgY was acquired by immunization of chickens with the yeast form, which was provided by GHEN Corporation (Tokyo, Japan) as a purified powder. A solution containing 4 mg/ml was prepared in PBS. Control IgY was prepared from the eggs of non-immunized hens. Fat-free egg yolk powder was purified for IgY using the ammonium sulfate precipitation method. The protein concentration was determined using the BioRad protein assay method (BioRad, Hercules, Calif., USA) based on the Bradford method. One milligram per milliliter of bovine serum albumin (IWAI, Tokyo, Japan) was used as the reference protein. The absorbance at 620 nm after a 30-min reaction with Bradford's solution was measured using a spectrophotometer.

Epithelial cells: The human oral squamous carcinoma cell lines, Ca9-22 and HSC-2, were purchased from the Japanese Collection of Research Bioresources in Health Science Research Resources Bank (Tokyo, Japan). They were maintained in Minimal Essential Medium Eagle's (SIGMA ALDRICH Corp., St. Louis, Mo., USA) containing 10% fetal bovine serum supplemented with 6 mg/ml L-glutamine, penicillin and streptomycin. They were grown on 24-well plates at 37°C in a humidified environment containing 5% CO_2 and used at 95% confluence in all experiments.

Antibody titration: Enzyme-linked immunosorbent assay (ELISA) was used to determine the titer of the specific antibody. Each well of a 96-well polystyrene plate was coated overnight at 4°C with 100 μl of whole yeast in PBS (OD_{660} = 1.0). The wells were washed with PBS-T (0.05% Tween 20 in PBS, PBS-T) and blocked with 150 μl 1.0% (w/v) skim milk in PBS-T for 1 h at 37°C. After three washes with PBS-T, various protein concentrations (0.032, 0.063, 0.125, 0.25, 0.5, 1.0, 2.0 and 4.0 mg/ml) of IgY were added to the wells; and the plates were incubated for 1 h at 37°C. The plates were washed three times, and alkaline phosphatase-conjugated goat IgG polyclonal anti-chicken IgY (ABCAM PLC, Cambridge, UK) in PBS-T (1:5,000 dilution) was added. After five washes with PBS-T, bound antibodies were detected after adding 100 μl of 3 mg/ml para-nitrophenyl phosphate as a substrate and incubating for 60 min at 37°C. The optical densities were determined using a microplate reader (Multiskan Bichromatic Laboratory Japan, Tokyo, Japan) at 405 nm. The background (control) was defined in wells coated without IgY. All samples were tested in triplicate.

Effects of anti-*C. albicans* IgY on cell growth of *Candida* strains: Cell suspensions of *C. albicans* SC5314 and 0 or 2 mg/ml of anti-*C. albicans* IgY or 2 mg/ml control IgY were mixed and incubated in YPD or PBS for 24 h at 37°C in aerobic conditions. The absorbance at 660 nm was measured at 0, 1, 3, 6 and 24 h after incubation. To confirm visually the specificity of the anti-*C. albicans* IgY, 2 mg/ml of anti-*C. albicans* and 2 mg/ml of control IgY were applied to cell suspensions of *C. albicans* SC5314 cultivated in YPD or RPMI1640 with 10% fetal bovine serum (FBS); and incubated aerobically for 60 min at 37°C. The cells treated with anti-*C. albicans* IgY and control IgY were washed three times using sterile PBS and mixed with 1/1,000 diluted FITC-conjugated rabbit anti-chicken IgY antibodies (ANASPEC, Sun Jose, Calif., USA) for 60 min at 37°C. The cells were washed three times using sterile PBS and observed using a confocal laser scanning microscope (Olympas, Tokyo, Japan).

Effects of anti-*C. albicans* IgY on adherence of *Candida* strains: Absorbance at 660 nm was measured to adjust the yeast concentration to OD_{660} = 1.0. The yeast was mixed with 0.006, 0.0125, 0.25, 0.5, 1 or 2 mg/ml IgY and 2 mg/ml control IgY for 60 min at 37°C and added to the epithelial cells on a 24-well plate. After 60-min incubation, yeasts adhering to the epithelial cells were separated from free yeasts by washing three times with PBS. Then, 1 ml 0.05% trypsin-EDTA was added to each well, and the plates were incubated for 10 min at room temperature. The detached cell suspensions were collected in 0.5% trypsin-EDTA using the pipetting technique, and spread on the YPD agar plate using an EDDY JET spiral plating system (IUL, S.A., Barcelona, Spain). After incubation for 24 h at 37°C under aerobic conditions, the number of colonies on the plates was counted and compared to those on the plates that did not have IgY.

Effects of anti-*C. albicans* IgY on biofilm formation of *C. albicans*: Biofilm formation by *C. albicans* SC5314 was assayed using a method described previously (28,29), with some modification. *C. albicans* incubated for 24 h at 37°C in YPD broth was adjusted to OD = 0.5 at 660 nm, harvested by centrifugation and washed in PBS two times. The *C. albicans* suspension was diluted with RPMI1640, and 2 mg/ml anti-*C. albicans* IgY was added to the 96-well microtiter plate wells. The chemically defined RPMI1640 medium containing minimal (0.2%) glucose with or without 10% FBS was used as the nutrient-poor condition for the biofilm formation assay. After incubation for 24 h at 37°C, biofilms formed in wells were washed with sterile PBS two times. Biofilm formation was tested using the XTT assay at 492 nm. XTT reduction has been widely used to measure biofilm activity and allows the detection of small differences in metabolic activity between strains (30-32).

Statistical analysis: All data were analyzed using the Statistical Package for SPSS for Windows (version 100; SPSS, Chicago, Ill., USA). The Student's *t* test with the Bonferroni Method was used to compare data of treatment with control IgY and anti-*C. albicans* IgY. *P*-values less than 0.05 were considered to be significant.

RESULTS

Antibody titers of IgY to *Candida* spp. were measured using ELISA (Fig. 1). Anti-*C. albicans* IgY reacted to *C. albicans* SC5314, *C. tropicalis* IFO0618, *C. dubliniensis* CD36 and CD57 in a dose-dependent manner where the IgY titers were significantly elevated at concentrations of 0.032, 0.073 or 0.125 mg/ml increasing to 4 mg/ml of antibody (IgY). By contrast, the control IgY to these *Candida* spp. were poor in all tested concentrations, whereas 4 mg/ml of the control antibody reacted only slightly to *Candida* spp. The titers of both antibodies were similar to those of other *Candida* strains (data not shown). Two milligrams per milliliters of IgY showed a stronger response to *Candida* strains than the control IgY and was used in further experiments. Before the *Candida* adherence tests, the effect of IgY was tested to determine whether the antibodies inhibited cell growth of *C. albicans*. Anti-*C. albicans* IgY did not inhibit the cell growth of *C. albicans* in comparison to the cell growth in YPD

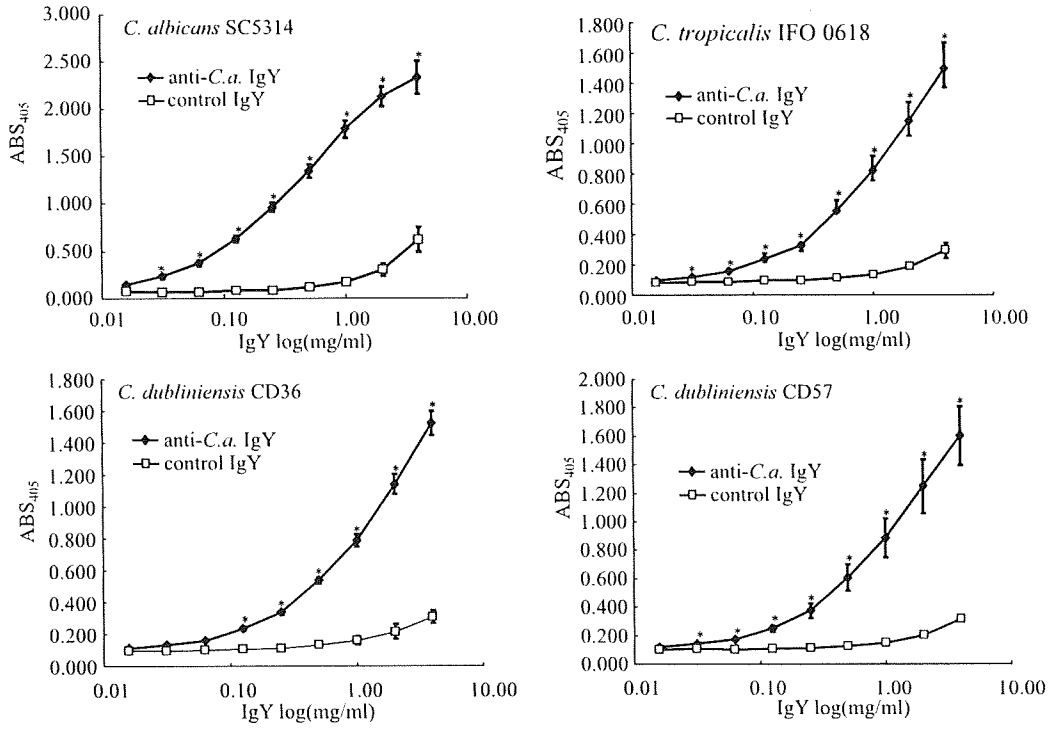

Fig. 1. ELISA antiboby titer of anti-*C. albicans* IgY. Various protein concentration (0.0, 0.063, 0.0125, 0.25, 0.5, 1.0, 2.0 and 4.0 mg/ml) of anti-*C. albicans* IgY or control IgY were applied to 96-well microtiter plates coated with *C. albicans* SC5314, *C. tropicalis* IFO0618, *C. dubliniensis* CD36 and CD57. The titers were determined using a microplate reader at 405 nm. Results are the mean ± standard deviation of three independent experiments each performed using triplicate assays; and compared to control IgY ($*P < 0.01$).

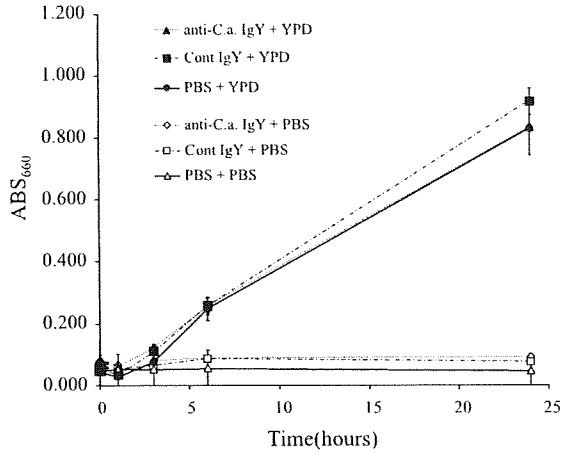

Fig. 2. Effects of anti-*C. albicans* IgY on *C. albicans* growth. Cell suspensions of *C. albicans* SC5314 were mixed with 0 or 2 mg/ml anti-*C. albicans* IgY or 2 mg/ml control IgY; and incubated in YPD or PBS for 24 h. The absorbance at 660 nm was measured at 0, 1, 3, 6 and 24 h after incubation. Results are the mean ± standard deviation of three independent experiments each performed using triplicate assays.

medium containing control IgY or PBS (Fig. 2). *C. albicans* did not grow in PBS containing anti-*C. albicans* IgY, control IgY and PBS. To confirm the reactivity of the anti-*C. albicans* IgY induced by immunization with the yeast form, a reaction assay using a second fluorescence-conjugated antibody was performed and observed by microscopy. The fluorescence activity did not appear in the assay using the control IgY (Fig. 3A). By contrast, significant fluorescence on the yeast form was confirmed using the anti-*C. albicans* IgY (Fig. 3B). Therefore, the reactivity of anti-*C. albicans* IgY to the *C. albicans* yeast form was confirmed. Further, the effect of anti-*C. albicans* IgY on the adherence of *Candida* spp. to monolayers of Ca9-22 epithelial cells was observed (Fig. 4). Anti-*C. albicans* IgY inhibited the adherence of *C. albicans* in a dose-dependent manner (from 0 to 2 mg/ml) whereas 2 mg/ml of control IgY and PBS did not inhibit the adherence. Further, anti-*C. albicans* IgY significantly inhibited the adherence of various *Candida* strains including different serotype strains (A and B) of *C. albicans* in comparison with control IgY (Fig. 5A). Inhibition of adherence was also observed in the other epithelial cell line, HSC-2 (Fig. 5B). To measure inhibition effects of anti-*C. albicans* IgY on biofilm formation of *C. albicans*, various concentrations of anti-*C. albicans* IgY were applied into the biofilm formation. Two milligrams per milliliters of anti-*C. albicans* IgY strongly inhibited the biofilm formation of *C. albicans* SC5314 in comparison with 2 mg/ml of control IgY (Fig. 6). Other concentrations of anti-*C. albicans* IgY did not affect the biofilm formation. Therefore, 2 mg/ml of anti-*C. albicans* IgY is a sufficient amount to inhibit biofilm formation. It is known that serum induces germ tube formation (filamentous form) in *Candida* (33). To detect the reactivity of the anti-*C. albicans* IgY to the germ tube, *C. albicans* was cultivated in medium supplemented with 10% FBS and mixed with the antibody. Yeast and filamentous forms were observed in Fig. 3C. The fluorescence activity of the filamentous form was lower than that of the yeast form of *C. albicans* in the assay using the anti-*C. albicans* IgY (Fig. 3C). To determine whether the IgY anti-*C. albicans* antibody affects the biofilm formation including the germ tube formation of *C. albicans*, we performed further experiments. The biofilm formation assay was performed in a medium conditioned with 10% FBS. Slight inhibitory activity by anti-*C. albicans* IgY was observed for the concentrations 0.25 and

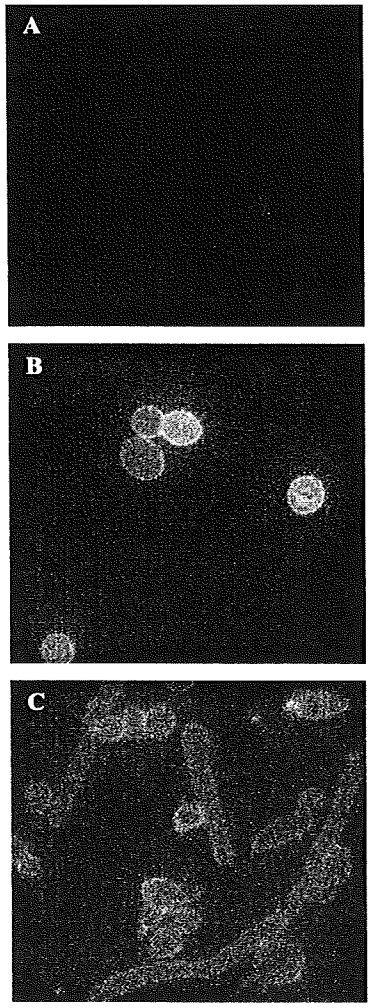

Fig. 3. Photograph of *C. albicans* with FITC-conjugated antibody. *C. albicans* SC5314 was treated with control IgY (A) or anti-*C. albicans* IgY (B). *C. albicans* formed germ tube was treated with anti-*C. albicans* IgY (C). After washing with PBS, the cells were mixed with FITC-conjugated rabbit anti-chicken IgY antibodies. Fluorescence photograph of *C. albicans* treated with antibodies were representative in three independent experiments.

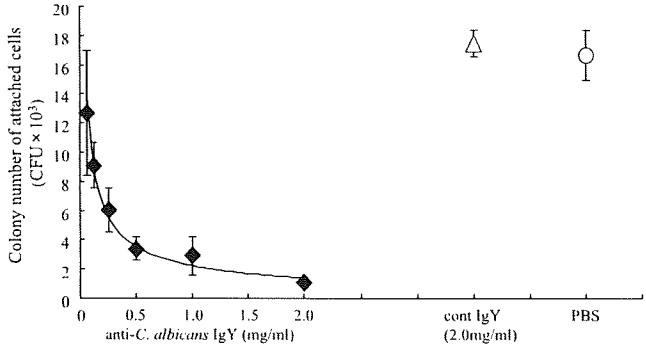

Fig. 4. Effects of anti-*C. albicans* IgY on *C. albicans* adherence. *C. albicans* SC5314 was mixed with 0.0, 0.063, 0.125, 0.25, 0.5, 1.0 and 2.0 mg/ml anti-*C. albicans* IgY, 2.0 mg/ml control IgY or PBS; and applied onto the epithelial cells (Ca9-22). The cell suspension detached using 0.05% trypsin-EDTA were spread on YPD agar plates. After incubation for 24 h, the numbers of colonies on the plates were counted. Results are the mean ± standard deviation of three independent experiments each performed using triplicate assays.

0.5 mg/ml ($P < 0.05$). The 2 mg/ml concentration of anti-*C. albicans* IgY significantly inhibited biofilm formation in the

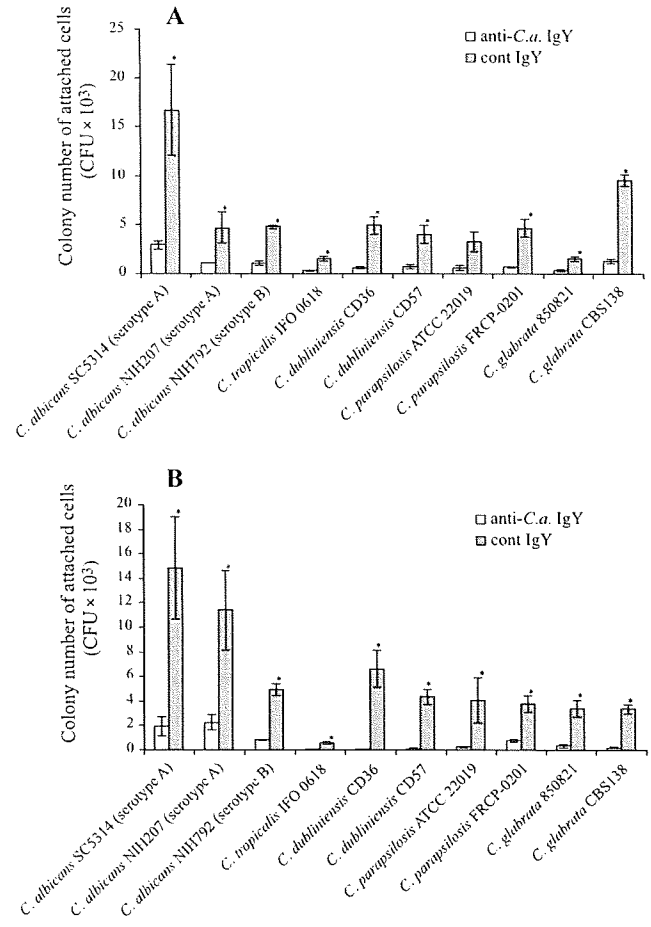

Fig. 5. Effects of anti-*C. albicans* IgY on *Candida* spp. adherence. *Candida* spp. were mixed with 2.0 mg/ml anti-*C. albicans* IgY or 2.0 mg/ml control IgY for 60 min. The treated cells were added onto monolayers of the epithelial cells {(A) Ca9-22 and (B) HSC-2}. The cell suspensions were detached using 0.05% trypsin-EDTA; and were spread on YPD agar plates. After incubation for 24 h, the numbers of colonies on the plates were counted. Results are the mean ± standard deviation of three independent experiments each performed using triplicate assays; and compared to control IgY (*$P < 0.01$).

medium with FBS ($P < 0.01$), but the inhibiting activity was weak in comparison with that by 2 mg/ml of anti-*C. albicans* IgY in the medium without FBS (Fig. 6). PBS did not affect biofilm formation in medium with or without FBS.

DISCUSSION

A number of secretory antibody-mediated mechanisms are operative in the mammary gland including (i) anti-adhesive activity, (ii) opsonization followed by phagocytosis, (iii) toxin neutralization and (iv) antibody-mediated lysis of pathogens (34). This study provided evidence for the anti-adhesive activity of anti-*C. albicans* IgY (IgA-like) against *C. albicans*. We found that anti-*C. albicans* IgY inhibits adherence of *C. albicans* and also other *Candida* spp. to monolayers of oral epithelial cells and confirmed that the IgY antibodies cross-reacted with various *Candida* spp. The IgY induced by immunization with *C. albicans* may react with various antigens including adhesins from *Candida* spp. that adhere to epithelial cells. For example, Hwp1 and Als3 are known for their role in host attachment and are the most well characterized *C. albicans* cell surface proteins (35,36). This is possibly the reason for the inhibition mechanism by anti-*C. albicans*

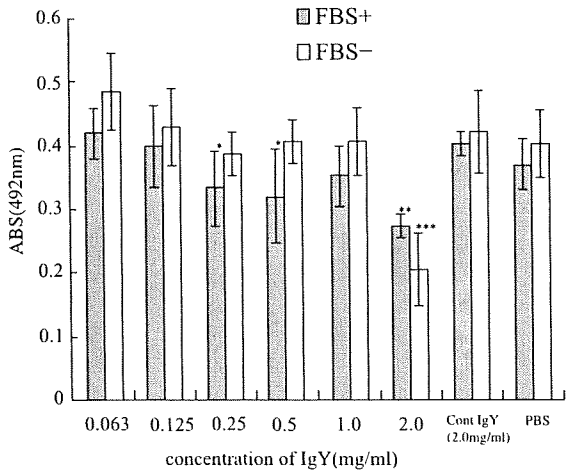

Fig. 6. Biofilm formation of *C. albicans* treated with anti-*C. albicans* IgY. A *C. albicans* SC5314 suspension was added to 0.0, 0.063, 0.125, 0.25, 0.5, 1.0 and 2.0 mg/ml anti-*C. albicans* IgY, 2.0 mg/ml control IgY or PBS to the wells of 96-well microtiter plates. After incubation for 24 h in PBS or YPD with and without 10% FBS, biofilm formation was observed using microphotography. Results are the mean ± standard deviation of three independent experiments each performed using triplicate assays; and compared to control IgY (*$P < 0.05$, **$P < 0.01$ in condition with FBS, ***$P < 0.01$ in condition without FBS).

IgY, where the IgY antibody may cross-react with adhesins Hwp1 and Als3 in the yeast form. The effects may also be associated with the inhibition of biofilm formation in the medium without conditioning serum.

However, the biofilm of *C. albicans* in the medium conditioned with 10% FBS was more resistant to anti-*C. albicans* IgY. A non-dialyzable component of serum induces germ-tube formation using the YPD medium supplemented with 10% serum (28,37). The inhibition of adhesion is usually achieved by blocking the adhesins present on the fungal cell wall (16), but for the inhibition of germination there may be another important mechanism because filamentation plays a key role in the adhesion process in biofilm formation (38). Anti-*C. albicans* IgY induced by immunization with the yeast form is not likely to play an extensive role in the germination of *C. albicans* since it may not include all antibodies to antigens of the filamentous form of *C. albicans* (Fig. 3C). Therefore, the germination might disturb the inhibition by anti-*C. albicans* IgY to biofilm formation in the presence of serum. In contrast to the discrete activity of germination and adhesion to the epithelial cells, anti-*C. albicans* IgY did not exhibit a potent fungicidal effect on *Candida* spp., as it did on *C. albicans*.

Passive immunization therapies against pathogens have been extensively studied (39-41). In the oral cavity, successful passive immunization with IgY against dental caries (e.g., *Streptococcus mutans*) has been reported in a rat model (42,43) and in human subjects (44). Oral passive immunization of anti-*C. albicans* IgY was shown to be effective (27) and significantly reduced the number of *C. albicans* colonies and the scores for tongue lesions. They indicated that this effect may be due to the blocking of the binding of *C. albicans* to the host cells. Here, we demonstrate that anti-*C. albicans* IgY has anti-adherence activity against various *Candida* spp. strains, both when grown in suspension and as a biofilm in the medium without serum. However, these concentrations of IgY did not achieve *Candida* growth inhibition. Chicken egg yolk immunoglobulin is recognized as an antibody source and showed therapeutic values against several microorganisms (19-26). It is possible the anti-*C. albicans* IgY may be used as a preventive immunotherapy against oral and disseminated candidiasis and *Candida* spp. infections. However, the IgY did not completely affect the biofilm formation when *C. albicans* formed germ tubes in the growth medium conditioned with serum. Therefore, treatment with anti-*C. albicans* IgY may be considered a prophylactic immunotherapy or possibly an adjunctive anti-fungal therapy under limited conditions.

ACKNOWLEDGMENTS

The authors thank Ryoma Nakao and Saori Yoneda for their technical support, helpful discussions, and advice.

This work was supported in-part by grants-in-aid for the Development of Scientific Research (15390571 and 18592011) and Exploratory Research (19659559) from the Ministry of Education, Culture, Sports, Science and Technology of Japan; and by a grant from the Ministry of Health, Labour and Welfare of Japan (H16-Medical Services-014 and H19-Medical Services-007).

REFERENCES

1. Odds, F.C. (1988): *Candida* and Candidosis. 2nd ed. Bailliere Tindall, UK.
2. Calderone, R.A. and Braun, P.C. (1991): Adherence and receptor relationships of *Candida albicans*. Microbiol. Rev., 55, 1-20.
3. Kumamoto, C.A. (2002): *Candida* biofilms. Curr. Opin. Microbiol., 5, 608-611.
4. Ramage, G., Saville, S.P., Thomas, D.P., et al. (2005): *Candida* biofilms: an update. Eukaryot. Cell, 4, 633-638.
5. Chandra, J., Patel, J.D., Li, J., et al. (2005): Modification of surface properties of biomaterials influences the ability of *Candida albicans* to form biofilms. Appl. Environ. Microbiol., 71, 8795-8801.
6. Kuhn, D.M., Chandra, J., Mukherjee, P.K., et al. (2002): Comparison of biofilms formed by *Candida albicans* and *Candida parapsilosis* on bioprosthetic surfaces. Infect. Immun., 70, 878-888.
7. Douglas, L.J. (2003): *Candida* biofilms and their role in infection. Trends Microbiol., 11, 30-36.
8. Baillie, G.S. and Douglas, L.J. (2000): Matrix polymers of *Candida* biofilms and their possible role in biofilm resistance to antifungal agents. J. Antimicrob. Chemother., 46, 397-403.
9. Chandra, J., Kuhn, D.M., Mukherjee, P.K., et al. (2001): Biofilm formation by the fungal pathogen *Candida albicans*: development, architecture, and drug resistance. J. Bacteriol., 183, 5385-5394.
10. De Bernardis, F., Boccanera, M., Adriani, D., et al. (1997): Protective role of antimannan and anti-aspartyl proteinase antibodies in an experimental model of *Candida albicans* vaginitis in rats. Infect. Immun., 65, 3399-3405.
11. Han, Y., Morrison, R.P. and Cutler, J.E. (1998): A vaccine and monoclonal antibodies that enhance mouse resistance to *Candida albicans* vaginal infection. Infect. Immun., 66, 5771-5776.
12. Matthews, R. and Burnie, J. (2001): Antifungal antibodies: a new approach to the treatment of systemic candidiasis. Curr. Opin. Investig. Drugs, 2, 472-476.
13. Eostein, J.B., Kimura, L.H., Menard, T.W., et al. (1982): Effects of specific antibodies on the interaction between the fungus *Candida albicans* and human oral mucosa. Arch. Oral Biol., 27, 469-474.
14. Fidal, P.L., Jr. (1999): Host defense oropharyngeal and vaginal candidiasis: site-specific differences. Rev. Iberoam Microl., 16, 8-15.
15. Vudhichamnong, K., Walker, D.M. and Ryley, H.C. (1982): The effect of secretory immunoglobulin A on the *in vitro* adherent of the yeast *Candida albicans* to human oral epithelial cells. Arch. Oral Biol., 27, 617-629.
16. San Millan, R., Elguezabal, N., Regulez, P., et al. (2000): Effect of salivary secretory IgA on the adhesion of *Candida albicans* to polystyrene. Microbiology, 146, 2105-2112.
17. Kuroki, M. (1999): Oral passive immunization using chicken egg yolk immunoglobulins against bovine rotavirus and coronavirus infection. Recent Res. Dev. Virol., 1, 95-106.
18. Akita, E.M. and Nakai, S. (1992): Immunoglobulins from egg yolk: isolation and purification. J. Food Sci., 57, 629-634.
19. Kuroki, M., Ikemori, Y., Yokoyama, H., et al. (1993): Passive protection against bovine rotavirus-induced diarrhea in murine model by specific immunoglobulins from chicken egg yolk. Vet. Microbiol., 37, 135-146.